The Geological Society of America
Special Paper 558

Geographically weighted regression in mineral exploration: A new application to investigate mineralization

Wenlei Wang
Institute of Geomechanics, Chinese Academy of Geological Sciences, 11 Minzudaxue South Road, Beijing 100081, China

Jie Zhao
Qiuming Cheng
State Key Lab of Geological Processes and Mineral Resources, China University of Geosciences (Beijing), 20 Chengfu Road, Beijing 100083, China

ABSTRACT

Geographically weighted regression (GWR) is an effective model for the investigation of spatially nonstationary relations among variables in the geographical and social sciences. GWR was introduced to the field of mineral exploration to further understanding of the location, controlling factors, and coupling mechanisms related to the triggering of mineralization—in other words, the where, what, and how. Previous studies reported that Cu and Au in a porphyry system present a paragenetic relation at different stages of mineralization, which can be an informative indicator in mineral exploration. As a successor, the current study further applies the GWR model to characterize the paragenetic relation between the ore-forming elements Cu and Au in the Duolong mineral district of Tibet, China, in a spatial scenario. Unlike the spatially varied ore-forming mechanism quantified by the regression coefficients of GWR, the coefficient of determination (R^2) is discussed to verify the existence and to evaluate the strength of the paragenetic relation between Cu and Au, because regression coefficients can only inform the mutual influence between one and the other. Furthermore, the fractal and multifractal-based spectrum–area method is adopted to separate the GWR results into anomaly and background. Areas with GWR results that indicate the existence and intensity of a paragenetic relation are mapped as target areas for mineral exploration. The current quantitative recognition of mineralization represents a meaningful and useful extension to the application and interpretation of the GWR model.

Wang, W., Zhao, J., and Cheng, Q., 2023, Geographically weighted regression in mineral exploration: A new application to investigate mineralization, *in* Ma, X., Mookerjee, M., Hsu, L., and Hills, D., eds., Recent Advancement in Geoinformatics and Data Science: Geological Society of America Special Paper 558, https://doi.org/10.1130/2022.2558(09).

INTRODUCTION

Mineral Exploration

The use of mineral resources in support of the development of human society has long been investigated. To narrow targeted areas and increase the possibility of success in the discovery and exploitation of mineral resources, specific exploration strategies from reconnaissance to ongoing exploration are usually planned and implemented systematically (Haldar, 2018; Hogson, 1990; Woodall, 1994). During the exploration stage, various practical investigation activities are conducted both in the field and in the laboratory to progressively improve geological knowledge in the areas of interest. Field-based geological surveys and related laboratory analyses have always been very important in providing the theoretical foundation for further interpretation of exploratory data sets. These data sets, widely derived from activities such as remote sensing, geological mapping, geophysical and geochemical exploration, and drilling, can be analyzed to detect mineralization-related anomalies (e.g., geoanomalies) and infer the possible existence and extent of mineralization. In practice, field-based surveys and laboratory analyses are mutually supportive; the former provide data that support interpretation, while the latter can identify anomalous areas with high mineral potential and metallogenetic mechanisms that can inform geological understanding derived from field surveys (Agterberg, 1989; Grunsky et al., 2014; Cheng, 2007; Wang et al., 2018; Zhao et al., 2013).

Geographic Information System-Based Mineral Exploration

Nowadays, geological signatures that reflect the evolution of the Earth system can be detected and analyzed to provide information regarding mineralization, geological disasters, and the geological environment. Broadly implemented geological surveys at continental and local scales (Darnley, 1995) have enhanced the construction of exploratory data sets considerably in terms of volume and quality. Through integration into geographic information system (GIS)-based analytical platforms, mathematical methodologies with high efficiency and practicability are available to assist in the analysis of diverse georeferenced exploratory data sets for improved understanding of complex natural systems (Agterberg, 1989; Bonham-Carter, 1994; De Paor, 1996). Usually, GIS-based investigations are conducted throughout all stages of mineral exploration. They can be applied not only in the reconnaissance stage to reduce the number and size of targeted areas (e.g., mineral prospectivity), but also in the ongoing stage to depict and evaluate potential ore bodies for mining (e.g., 3-D modeling). In modern mineral prospectivity modeling, geoanomalies associated with mineralization are often identified and further integrated within a GIS environment to illustrate mineralization-favored areas or spaces, which is a process known as geoinformation extraction and integration (Bonham-Carter, 1994; Wang et al., 2011).

In geoinformation extraction, geoanomalies that are indicative of mineralization and/or its controlling factors are often identified from observational data sets. Over previous decades, numerous geoanomaly extraction methodologies have been proposed and discussed. Such methodologies often include statistical approaches that are based on the hypothesis that mineralization-related geovariables (i.e., geochemical data) follow a normal or lognormal distribution (Ahrens, 1953). A simple but classical treatment for separating geoanomalies from the background is through use of the algorithm of the mean ± standard deviation(s) according to the lognormal (normal) distribution of geovariables. Furthermore, spatial statistical approaches can assist in determination of the optimal spatial correlation between mapped geological features (e.g., fault traces and outcrops of intrusions) and mineral occurrences discovered (Bonham-Carter, 1994), by which mineralization-favored spaces produced by tectonomagmatic activities can be delineated. In geoanomaly integration, application of multistatistical methods is important and necessary in many cases. For example, geochemical data recording concentrations of multiple elements or compounds should be analyzed using cluster or factor analysis methods (Grunsky, 1986; Grunsky and Smee, 1999; Grunsky et al., 2009; Cheng et al., 2011; Zhao et al., 2016). This is because, unlike multivariates or multiple element associations, single elements or univariates are inadequate for representing the general geochemical background of an explored area. Moreover, geoanomalies that are indicative of various aspects of mineralization can be further integrated through use of the weighted overlay theory (Carranza and Hale, 2002; Cheng et al., 2011). Depending on the principles used to define the weights, the weighted integration is generally sorted into data-driven (Harris et al., 2003), knowledge-driven (An et al., 1991), and hybrid (Cheng and Agterberg, 1999) modeling.

After a century of seeking knowledge, scientists have recognized that the real world may be essentially nonlinear (Ghil, 2019). Because of the limitations of inadequate capability and means of cognition, nonlinear natural phenomena have often been explicated linearly. The linearization process simplifies a complex nonlinear system into several linear subsystems that are then investigated using statistical methods. However, linearization commonly applied in mineral exploration (Agterberg, 2007; Cheng, 2007) is not always fully realized, especially when the linear subsystems are unable to characterize real situations adequately. The potential interpretation is that the normal or lognormal distribution of geovariables may only be efficient for solving linear problems. However, the hypothesis would be invalid for cases corresponding to or informative of mineralization-related nonlinear processes (Cheng et al., 1994). Among various progressive developments in nonlinear theory and methodology, fractal and multifractal methods (Cheng et al., 1994; Xu and Cheng, 2001; Xie and Bao, 2004) have been well developed and applied broadly to characterization of the spatial distributions of mineralization-related geoanomalies. Taking both frequency distributions and spatial self-similarity into consideration, fractal and multifractal methods produce informative anomalous patterns that are more indicative of mineralization. Typical examples of fractal and multifractal methods include the number–size model (Mandelbrot, 1983), concentration–area model, perimeter–area model (Cheng et al., 1994), spectrum–area model (Xu and Cheng, 2001), concentration–distance model (Li et al., 2003), multifractal singular value decomposition model (Li and Cheng, 2004), and singularity theory (Cheng, 2007). In recent years, even more fractal models have been proposed, e.g., the co-simulated size–number model (Madani and Carranza, 2020), global simulated size–number model (Madani and Sadeghi, 2019), concentration–distance from centroids model (Sadeghi and Cohen, 2021a), category-based fractal model (Sadeghi and Cohen, 2021b), and concentration–concentration model (Sadeghi et al., 2021). These earlier exploratory studies well demonstrated the quantitative and qualitative identification and characterization of mineralization-related spatial and frequency properties from multisource observational data sets. Moreover, certain weak anomalies that are difficult to distinguish from the background using linear statistics, owing to the buried depth and irregular shapes of causative geological bodies, were successfully enhanced and separated (Cheng, 2007, 2012; Zhao et al., 2012; Zuo et al., 2009).

New Opportunities

Over the centuries, academic and industrial communities have contributed continuously to mineral exploration, and most exposed or shallow buried deposits have been discovered and exploited. Thus, in the search for additional new discoveries, mineral prospecting has focused increasingly on covered spaces that are deeper. However, opportunities and difficulties go together, just as hope and challenges coexist. It is foreseeable that potential deposits at depth will be mostly concealed and rarely exhibit surficial signatures (Pirajno, 2009). In addition to improved geological knowledge regarding mineralization at depth, development of both advanced observational technologies and effective methods for analysis and processing of exploratory data could represent the direction of future mineral exploration.

Introduced by Mayer-Schönberger and Cukier (2013), the concept of big data has brought a new paradigm to both the natural and social scientific communities. Also known as the fourth paradigm (Mayer-Schönberger and Cukier, 2013), it defines a new generation of technological frameworks with a high capacity to capture, discover, and analyze complex and mass data to mine useful information or even knowledge. One example of these advances is the utilization of cluster analysis, factor analysis, artificial intelligence, and other machine learning algorithms to find or dig out correlations among various data sets that used to be known as independent or weakly associated, which then gradually became key to breakthroughs in seemingly unsolvable issues of the day.

Mineral exploration faces new opportunities and challenges regarding detection capability, data analysis efficiency, and integration of multisource heterogeneous data (Zuo et al., 2019; Zuo, 2020). In situations where traditional exploration theory and technology may be impracticable for locating and assessing ore bodies buried at depth, it is crucial to introduce new technologies and methods that could deeply mine and accurately interpret geoanomalies that indicate mineralization at different scales. Identified patterns should be meaningful and supportive to trigger new ideas or directions for mineral exploration in both the industrial and academic communities.

New Challenges

The origin, formation, and evolution of mineralization within the Earth system occur through nonlinear dynamic geoprocesses (Cheng and Agterberg, 2009). Taking endogenic deposits as an example, coupling mechanisms among tectonomagmatic and other related geological activities are believed to be among the causative issues that most affect the occurrence of mineralization (Pirajno, 2009). The varied and heterogeneous ore-forming mechanisms with discontinuity, nonstationarity, and irregularity in spatiotemporal scenarios can consequently cause diversity in the type of mineralization, zonation of alterations, differentiation of grade-tonnage, and gradient of formation depth. Physicochemical signatures of controlling factors (e.g., faults, folds, intrusions, and ore-bearing strata), which are formed and continuously deformed in the premineralization, synmineralization, and postmineralization stages, always present apparent or gradual differences from their surroundings that can be recorded in ground- and aero-based observational data sets. Geoanomalies identified from these multisource data sets that demonstrate distinctive patterns across the space consequently indicate and inform the spatially varied mechanism. Specifically, intrinsic associations and/or correlations among geoanomalies that appear seemingly unrelated could potentially enhance or even overturn current cognition and assumptions regarding mineralization (W. Wang et al., 2015a).

In many cases, the geoanomalies identified could be less useful interpretatively, not only because of the quality of the analytical methods or data sets, but also because of limitations in cognition and knowledge of the day. However, it remains reasonable to expect that anomalous patterns could be identified using data-driven methods and interpreted by specialists to evaluate the possibility of finding breakthroughs in mineral exploration (Carranza, 2009). The current study introduces the geographically weighted regression (GWR) model (Brunsdon et al., 1996) and its recent application to mineral exploration. Results of a new case study regarding application of this model in the Duolong mineral district of Tibet, China, are presented to characterize spatially nonstationary relations between ore-forming elements. Additionally, a fractal- and multifractal-based method is utilized to further identify informative patterns that could support new discoveries in this area.

GEOGRAPHICALLY WEIGHTED REGRESSION (GWR)

Heterogeneous and nonstationary correlations among diverse spatial data are recent areas of interest in the field of spatial statistics (Brunsdon et al., 1996; Fotheringham et al., 2002). Characterization of the spatial variation of parameters can well satisfy pursuit of the physical meaning of heterogeneous data structures in geographical and environmental studies (Lu et al., 2014; Tu and Xia, 2008). Brunsdon et al. (1996) applied a weighted regression model to analyze spatial data at different locations and further used local regression parameters to reveal nonstationary structures recorded within the data. Subsequently, the GWR method was developed and flourished in many fields of application, and it has become an important modeling method with which to investigate spatially nonstationary relations.

GWR Basics

The ordinary least squares regression model can be used to evaluate the relation between independent and dependent variables:

$$y = \beta_0 + \sum_{k=1}^{m} \beta_k x_k + \varepsilon_i, \tag{1}$$

where β_0 is the intercept, β_k is the regression coefficient of the k^{th} independent variable, and ε_i is the residual at location *i*. The value of β_k, which is a constant regardless of the spatial variation, can only represent general or global causality rather than support detailed interpretation of the causes of practical issues at the local scale. Unlike the ordinary least squares model, the GWR model can be used to investigate local relations among variables at different locations and provides a more localized expression. Following Lu et al. (2020), the basic model can be expressed as follows:

$$y_i = \beta_0(u_i, v_i) + \sum_{k=1}^{m} \beta_k(u_i, v_i) x_{ik} + \varepsilon_i, \tag{2}$$

where y_i, x_i, and (u_i, v_i) represent the dependent variable, independent variables, and geographic coordinates at location *i*, respectively; $\beta_0(u_i, v_i)$ is the intercept; $\beta_k(u_i, v_i)$ is the regression coefficient of the k^{th} independent variable; and ε_i is the residual. The regression coefficients of the independent variables at location *i* can be estimated as follows:

$$\beta_k(u_i, v_i) = (X^T W(u_i, v_i) X)^{-1} X^T W(u_i, v_i) Y. \tag{3}$$

The key factor to realization of local estimation of the spatially varied relationships among geovariables is the geographical or spatial weighting matrix *W*:

$$W_i = \begin{matrix} W_{i1} & 0 & \cdots & 0 \\ 0 & W_{i2} & & 0 \\ \vdots & & \ddots & \vdots \\ 0 & 0 & \cdots & W_{in} \end{matrix} \tag{4}$$

where the diagonal parameters $W_{in} \in [0,1]$ represent the weights of observed samples within a certain distance from location *i*, (u_i, v_i). A basic criterion regarding definition of the weights is that the closer the distance, the higher the given weight. Generally, a number of functions are available for defining the weights:

(1) Gaussian function

$$W_i = e^{\frac{(d_{ij}/b)^2}{2}} \tag{5}$$

(2) Exponential function

$$W_i = exp\left(-\frac{|d_{ij}|}{b}\right) \tag{6}$$

(3) Boxcar function

$$W_i = \begin{Bmatrix} 1, d_{ij} \le b \\ 0, others \end{Bmatrix} \tag{7}$$

(4) Bisquare function

$$W_i = \begin{cases} (1 - (d_{ij}/b)^2)^2, d_{ij} \le b \\ 0, others \end{cases} \tag{8}$$

(5) Tricube function

$$W_i = \begin{cases} (1 - (d_{ij}/b)^3)^3, d_{ij} \le b \\ 0, others \end{cases} \tag{9}$$

In the above, *b* is the bandwidth that defines a local area within which observed samples are analyzed to estimate the regression coefficient $\beta_k(u_i, v_i)$ at calibration location *i*, and d_{ij} is the distance of the n^{th} observed sample from calibration location *i* within the defined area. Applying the regression for each location across the space produces the spatial distribution of intercept $\beta_0(u_i, v_i)$, a set of regression coefficients $\beta_k(u_i, v_i)$, and the residuals ε_i. Further discussion regarding selection of these functions can be found in many recent publications by Professor Alexander Stewart Fotheringham of Arizona State University (see, for example, Brunsdon et al., 1996; Fotheringham et al., 2002; and Lu et al., 2014).

Bandwidth *b* is an important parameter regarding weight definition that has two types: fixed and adaptive. A fixed bandwidth means that a certain distance is predefined for estimation of regression coefficients for all *i* locations across the space. Determining local ranges for analysis would be a reasonable approach that experts might take if observed samples are locally insufficient owing to uneven distribution. An adaptive bandwidth allows the number of samples neighboring calibration point *i* or the regression distance from different calibration points to vary across the space. In this situation, the adjustable bandwidth ensures that the same number of samples is utilized for the regression at all *i* locations. Fixed and adaptive bandwidths both have predefined distances and sample sizes that determine the scale of investigation. A long (short) distance and a large (small) number of samples will lead to regional (local)-scale estimation of correlation. Thus, bandwidth definition should be treated with caution because an inappropriate bandwidth setting may lead to underfitted or overfitted estimation.

The spatial distributions of the residuals ε_i and R_i^2 are two other important parameters for evaluating GWR results. As a measure of differences between observed and predicted values, small residuals reflect significant regression effects. If the randomness of spatially distributed residuals can be proven using the Moran's *I* value, then the selection of dependent variables in the GWR model can be considered as appropriate, and consequently the results will be stable. In considering R_i^2 as another indicator for evaluating the quality of a regression model, the higher the value of R_i^2 ($R_i^2 \in [0,1]$), the better the result of the achieved regression. Thus, spatial distributions of regression coefficients $\beta_k(u_i, v_i)$ can consequently be accepted and interpreted. Further discussion regarding these critical parameters and the selection of weighting functions can be found in many recent studies of GWR and related case studies (Lu et al., 2020).

GWR in Mineral Exploration

After more than two decades, the concept and theory of GWR have become important research topics, not only in the field of geography but also in other areas such as the environment, social science, and geology. Numerous studies have contributed to this progress by reporting modeling algorithms, crucial parameters, and application scenarios of GWR (Lu et al., 2020). In the context of the current study, previous applications of GWR in the field of mineral exploration are reviewed briefly.

As introduced above, mineralization is a nonlinear dynamic geoprocess controlled substantially by coupling mechanisms of various factors. Occurrences of controlling factors such as tectonomagmatic and sedimentary activities are not always spatiotemporally homogeneous. Therefore, coupling mechanisms may vary spatially, and the metallogenetic model of explored mineralization could consequently be nonstationary. On the basis of this hypothesis, the spatial variation of controlling effects of faults, wall rocks, and intrusions on hydrothermal mineralization were investigated using the GWR model (Zhao et al., 2013, 2014; W. Wang et al., 2015a). It should be clarified that information regarding mineralization, faults, wall rocks, and intrusions is not collected from observations directly. These independent and dependent variables need to be established on the basis of geoinformation extraction and integration (W. Wang et al., 2015a). Application of GWR in mineral exploration can be considered as successor to or development of GIS-based mineral exploration. Thus, controlling effects of faults, wall rocks, and intrusions can be well characterized spatially (Zhao et al., 2013, 2014; W. Wang et al., 2015a). Such results provide more detailed understanding regarding the location (where), controlling factors (what), and coupling mechanisms (how) related to the triggering of mineralization.

Appropriate interpretation can improve understanding of local metallogeny and be used to guide subsequent stages of mineral exploration. Moreover, the concept of geographically weighted statistics has been discussed and applied to characterize mineralization-related geochemical patterns (H. Wang et al., 2015). On the basis of previous experience, the GWR model described in this chapter was applied to investigate the spatial variation of the paragenetic relation between two ore-forming elements, which are further utilized as a novel indicator for new discoveries in the study area.

CASE STUDY

Study Area

The study area of the Duolong mineral district in northern Tibet, China, is located on the southern rim of the southern Qiangtang terrane and in the northern part of the Bangongco–Nujiang (Bannu) suture zone (Fig. 1). This new mineral district with encouraging Cu-Au discoveries demonstrates huge resource potential and exploration value (Li et al., 2017). Mineral deposits discovered there comprise porphyry Cu-Au and high-sulfidation epithermal Cu-Au (Fig. 1). The area has 10 typical deposits and mineralized prospects called Duobuza, Gaerqin, Bolong, Tiegelong, Tiegelongnan, Naruo, Saijiao, Sena, Nadun, and Dibao (Table 1; Lin et al., 2019; Song et al., 2018). Mineralization and its related tectonomagmatism were highly affected by the evolution of the Bannu oceanic basin from its initial opening stage during the Early Permian (Zhu et al., 2016) or Middle–Late Triassic to Early Jurassic (Pan et al., 2012), expansion and subduction of the ocean floor in the Middle–Late Jurassic attributable to the assembly of the Lhasa and Qiangtang terranes (Zhang et al., 2015; Zhu et al., 2016), and the final closing stage during the Early–Late Cretaceous (Fan et al., 2014; Xu et al., 2014).

Evidence from geochronological analysis indicates that ore-bearing granodiorite and granite porphyries were coeval with the closure of the Bannu Basin (Song et al., 2018). Multistage tectonism consisting of structural compression, strike-slip, and stretching markedly influenced the structural framework and mineralization. The EW-, NE-, and NW-trending faults produced during different evolutionary stages of the Bannu Basin further controlled the formation and spatial distribution of mineralization (Song et al., 2018). The NE- and NW-trending, strike-slip faults (F5–F10 and F11–F14) demonstrate conjugated and mesh-like patterns formed during premineralization or synmineralization. The EW-trending reverse faults (F1–F4) formed in the postmineralization stage substantially broke and reshaped the ore bodies that can be observed from borehole samples. The stratigraphic sequence from old to young in this area comprises limestones of the Upper Triassic Riganpeicuo Formation (T_3r); the Cu-Au ore-bearing Lower Jurassic Quse Formation (J_1q); the Cu-Au ore-bearing Middle Jurassic Sewa Formation (J_2s) composed of flysch or flysch-like sediments; the Lower Cretaceous Meiriqiecuo Formation (K_1m) composed of continental-facies, intermediate–basic volcanic rocks; the Upper Cretaceous Abushan Formation (K_2a); and the upper Oligocene Kangtuo Formation (E_3k).

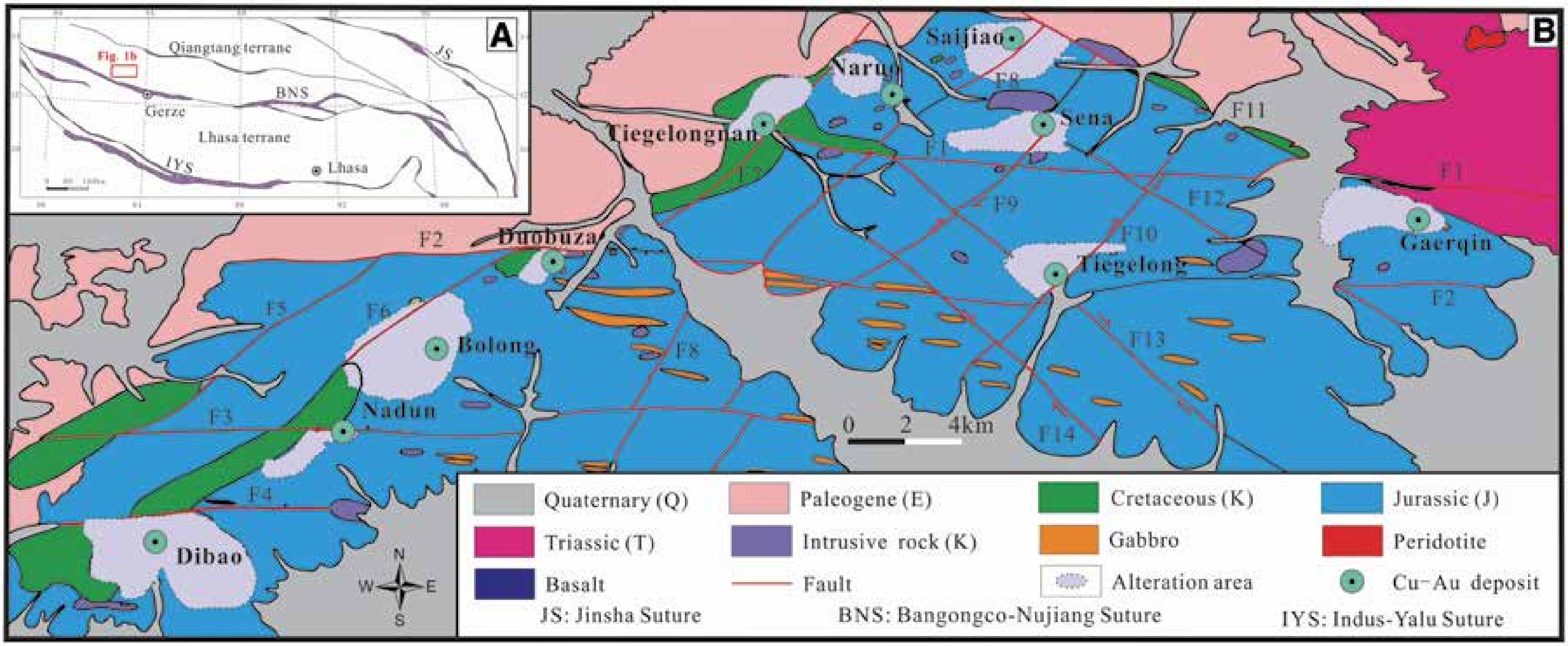

Figure 1. (A) Location map shows the study area (modified from Hou et al., 2006). (B) Simplified geological map (1:500,000 scale) of the Duolong mineral district, Tibet, China (modified from Wang et al., 2017).

TABLE 1. CHARACTERISTICS OF PORPHYRY COPPER SYSTEM IN DUOLONG DISTRICT, TIBET (AFTER LIN ET AL., 2019)

Deposit	Mineralization	Metal Cu(Mt); Au(t)
Dibao	High sulfidation epithermal Cu(Au) Porphyry Cu	Cu: 0.1; Au: 8
Nadun	High sulfidation epithermal Cu(Au) Porphyry Cu	N/A
Bolong	Porphyry Cu(Au)	Cu > 3.7; Au > 178
Duobuza	Porphyry Cu(Au)	Cu > 2.9; Au > 90
Tiegelongnan	High sulfidation epithermal Cu(Au) Porphyry Cu (Au)	Cu > 10; Au > 37
Naruo	Porphyry Cu(Au)	Cu > 2.5; Au > 80
Sena	High sulfidation epithermal Au	Mineralized prospects
Saijiao	High sulfidation epithermal Au	Mineralized prospects
Tiegelong	Porphyry Cu(Au)	Mineralized prospects
Gaerqin	High sulfidation epithermal Au	Mineralized prospects

N/A—not applicable.

Recent GIS-Based Mineral Exploration

Among discovered mineral deposits in the Duolong mineral district, the mineral occurrences explored are mainly gathered in certain local ore fields, e.g., the super-giant Tiegelong and Naruo deposits. Because of the substantial reserves, the general short-term exploration strategy adopted in this region is to undertake continuous exploration of these two deposits at depth (Yu et al., 2019) and seek new discoveries in other places (Liu et al., 2017; Liu et al., 2020). Within this context, exploratory data sets have been further analyzed and broadly discussed to identify new targets with giant mineral potentials. Through integration of ore-forming elements with indicator elements of fault activity, Wang et al. (2017) inferred a mesh-like structural framework and considered its controlling effects on porphyry mineralization. Subsequently, their findings were further used as indirect and/or proxy geoinformation to support mineral exploration in the Duolong mineral district. Liu et al. (2017) applied fractal- and multifractal-based methods to separate anomalies from the background of the main ore-forming element Cu and then used the mesh-like patterns identified as supplementary information to illustrate a tectonic framework suitable for producing spaces favorable for porphyry pluton emplacement and porphyry mineralization (Fig. 2). Yu et al. (2019) applied 3-D modeling methods to investigate geological, geochemical, and geophysical data of the Tiegelongnan deposit and identified mineralization-related anomalies at depth. Liu et al. (2020) utilized a knowledge-driven approach to further analyze geochemical data and circled two potential areas of interest based on statistical results.

Paragenetic Cu-Au Relation

Mineralization-associated geoanomalies should be investigated systematically using data mining technology to quantitatively characterize and qualitatively interpret informative patterns by which knowledge regarding the spatial distribution of mineralization could be enhanced in support of new discoveries in the study area. Within porphyry deposits, Cu and Au are highly correlated from the mineral-grain scale (textural intergrowth) to the ore-sample scale (characteristic Au/Cu ratios). Ulrich et al. (1999) utilized laser ablation–inductively coupled plasma–mass spectrometry to determine the Cu and Au concentrations of single fluid inclusions in quartz sampled from two of the world's largest Cu/Au deposits. Their results well demonstrated that the Au/Cu ratio of primary high-temperature brines is identical to the bulk Au/Cu ratio. On the basis of this finding, it was concluded that Cu and Au should be cotransported in fluids and coprecipitated in ore bodies when deposits are formed (Ulrich et al., 1999).

Among the 10 mineral deposits and mineralized prospects discovered in the Duolong mineral district, numerous sampling and laboratory analysis studies have been conducted using cores, thin slices, scanning electron microscopy, and geochemical analysis (Fan et al., 2014; Xu et al., 2014; Zhang et al., 2015; Zhu et al., 2016). To demonstrate the paragenetic relation between Cu and Au in the study area, concentrations of these two elements were derived from typical boreholes in the Rongna and Tiegelongnan deposits. In this test, the least squares regression method was applied to examine the Cu and Au concentrations of six boreholes. Regression coefficients calculated using all six sets of data indicate positive correlations between Cu and Au, although the shapes of scatters differ markedly from one another. Owing to outliers, it is remarkable to see that most linear relationships present low values of R^2 (Figs. 2C–2F), which indicates correlation that is not as strong as that in RNGZK0001 (Fig. 2A) and RNGZK0804 (Fig. 2B); however, the existence of paragenetic relations between Cu (vertical axis) and Au (horizontal axis) can still be determined from the general trends (Fig. 2). If one takes the distribution of outliers into account, despite the main trend demonstrated by the regression line, the divergence in multiple directions cannot be ignored. In other words,

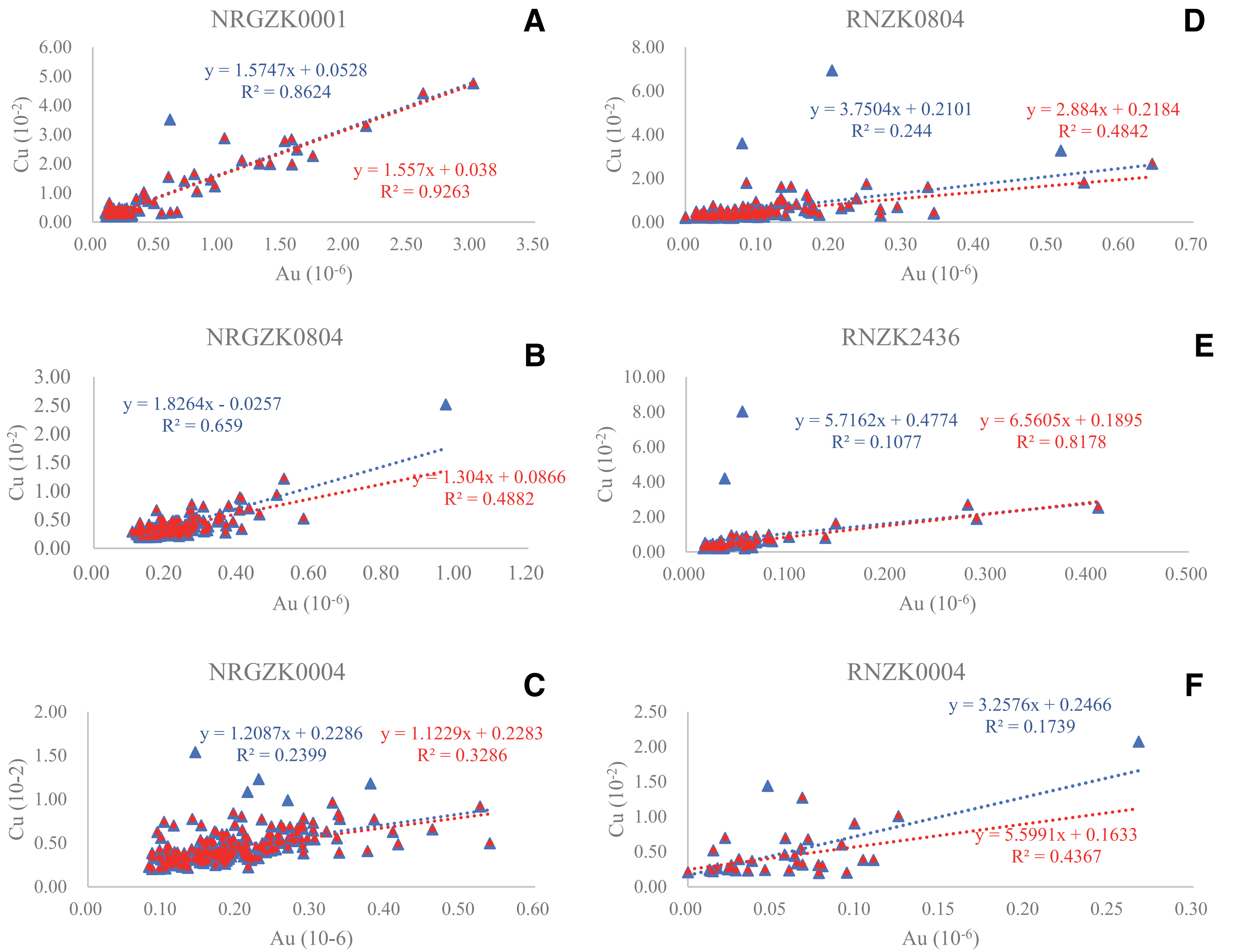

Figure 2. Relations between ore-forming elements Cu and Au are plotted. Cu and Au concentrations were collected from sections of ore bodies revealed by boreholes: (A) NRGZK0001, (B) NRGZK0804, and (C) NRGZK0004 are from the Naruo deposits; (D) RNZK0804, (E) RNZK2436, and (F) RNZK0004 are from the Tiegelongnan deposits.

although these sample points exhibit different linear or even nonlinear relations, a principal trend is evident. It is speculated that although Cu and Au may coexist in various ways, they still follow a predominant paragenetic relation. Consideration of all six boreholes reveals that trends of the pattern of scatters along different directions are not unique. Thus, it can be inferred that the paragenesis between Cu and Au presents spatial nonstationarity in both 2-D and 3-D scenarios.

It is evident that least squares regression is not sufficiently powerful to examine the nonstationary paragenetic relations between elements across the space; only the general trend can be identified rather than local variability. To elicit better understanding of the spatially nonstationary relation between Cu and Au in the study area, the GWR method was further applied to investigate this issue for mineral exploration.

Data Analysis and Results

Exploratory Data and Preliminary Recognition

In this chapter, 1:500,000-scale geological and geochemical data are utilized. Geological data comprising locations of discovered mineral deposits and fault traces from a geological mapping database are used as reference or verification for analytical results. Geochemical data collected from drainage basins constitute 3217 sedimentary samples from streams (Fig. 3) with 500 m spatial resolution based on a sampling density of four samples/km^2 (Wang et al., 2017). Concentrations of 15 trace elements in each sample were determined by X-ray fluorescence spectrometry (for Cu, Pb, Zn, Cr, Ni, and Mn), catalytic polarography (for Mo and W), atomic fluorescence spectrometry (for As, Sb, Bi, and Hg), emission spectrometry (for Ag and Sn), and graphite furnace

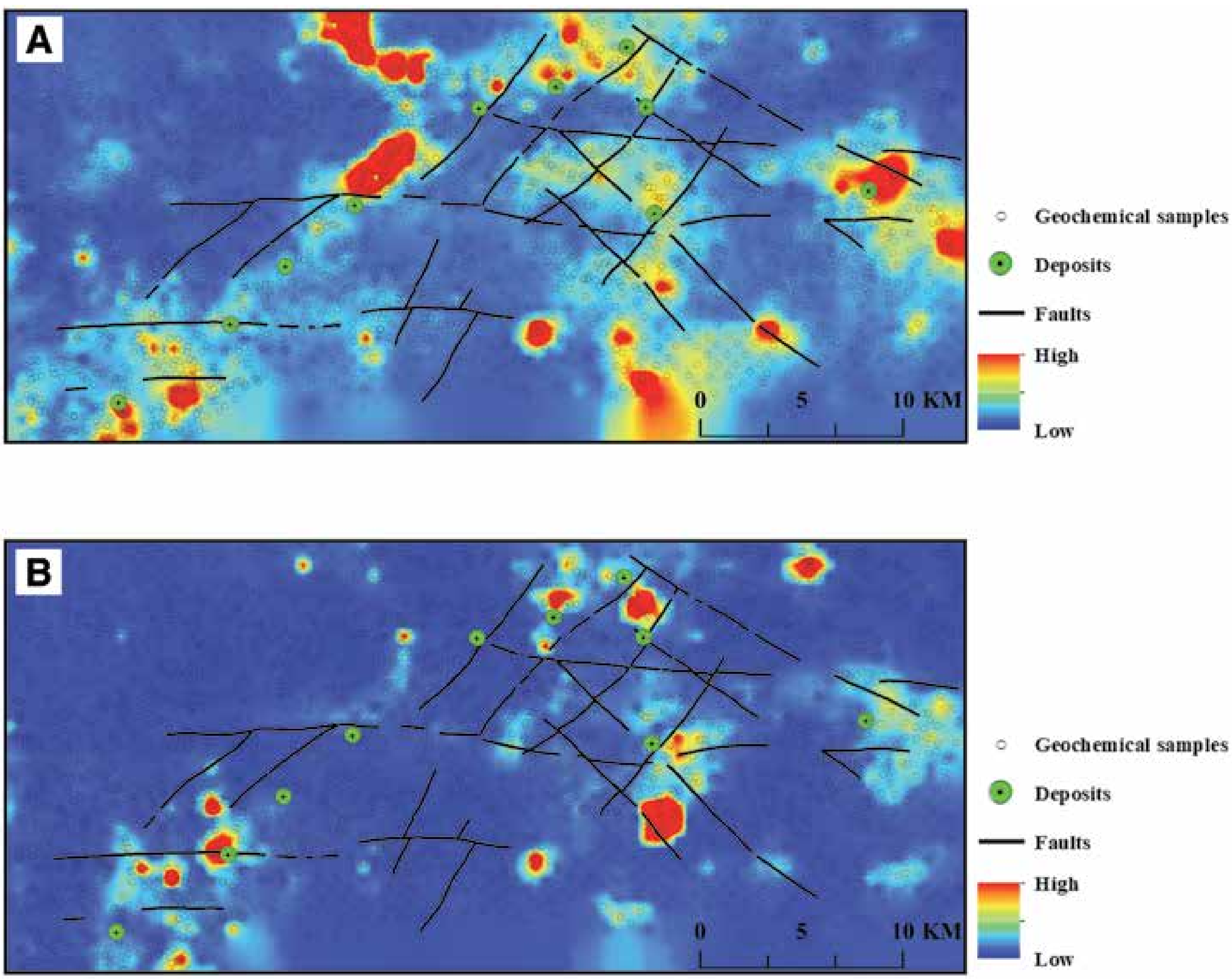

Figure 3. Spatial distributions of ore-forming elements (A) Cu and (B) Au in the Duolong mineral district, Tibet, China (modified from Wang et al., 2017) are plotted. Patterns in red indicate high concentration values, and patterns in blue indicate low concentration values; hollow circles represent geochemical sampling sites.

atomic absorption spectrometry (for Au). Further discussion of the geochemical data and additional details regarding analytical accuracy and precision can be found in Wang et al. (2017).

As introduced above, GIS-based mineral exploration in the Duolong mineral district was conducted. Using various advanced spatial analytical methods, distributions of geochemical signatures were analyzed rigorously. Not only have concentrations of ore-forming elements Cu and Au (Wang et al., 2017) been depicted (Figs. 3–4), but all 15 elements were also integrated (Liu et al., 2017) to comprehensively delineate the general geochemical background of the study area (Fig. 5). From geochemical distributions of Cu, Au (Fig. 3), and the elemental association (Fig. 5A), several isolated anomalies, distributed from the central south to the southeast of the study area, cannot be interpreted properly because they do not match the locations of any mineral deposits discovered and/or mapped controlling factors (e.g., faults and porphyries) that could be used to verify or explain the rationality of their existence. For this reason, previous studies (Wang et al., 2017; Liu et al., 2017) applied a fractal and multifractal-based spectrum–area model (Xu and Cheng, 2001) to separate anomalies from background geochemical distributions, and a mesh-like structural framework was interpreted on the basis of two groups of linear anomalous patterns trending in NE and SW directions (Fig. 4B). Utilizing the student's *t*-value in the weights-of-evidence method (Bonham-Carter et al., 1989), the spatial association of geochemical anomalies with deposits

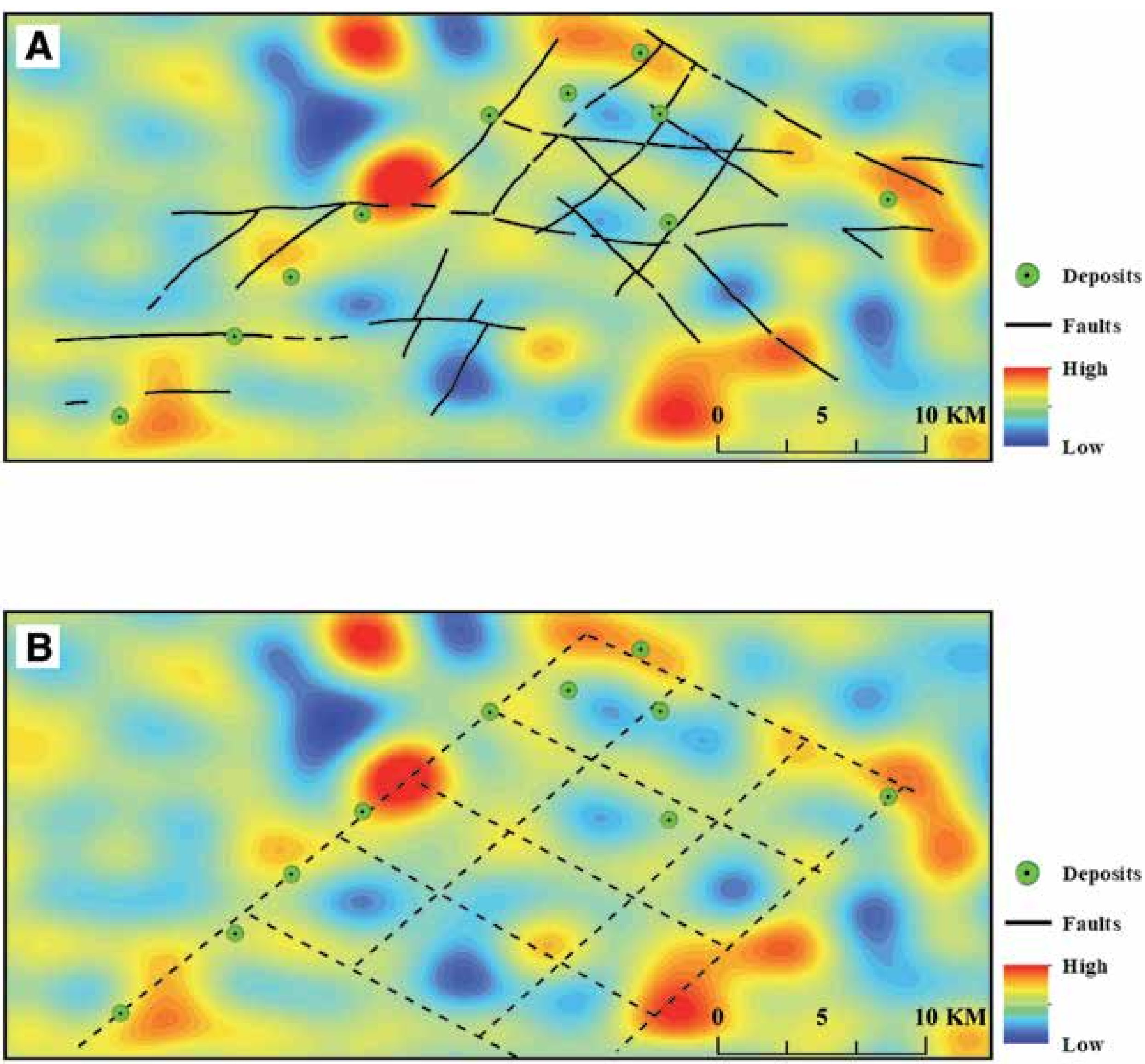

Figure 4. Background patterns of Cu concentrations are overlapped by (A) fault traces and (B) structural framework identified by Liu et al. (2017).

discovered and intersections of inferred faults were evaluated (Fig. 5C). Consequently, areas with the highest association (i.e., highest *t*-value) between mineralization and inferred fault intersections could be depicted (Fig. 5D). Thus, these beaded and isolated anomalies that match perfectly with intersections of interpreted linear structures trending along different directions in a mesh-like pattern become explainable and reasonable in the context of the geological background. Therefore, they were defined as potential areas worthy of further detailed exploration. All of these data-driven analyses contributed new geoinformation and supportive knowledge regarding the poorly identified structural framework in the study area, the results of which are consistent with the theory that strike-slip fault discontinuities (intersections) with high shear stress are favorable zones for porphyry pluton emplacement and porphyry mineralization (Segall and Pollard, 1980; Carranza and Hale, 2002). Supplementing mapped fault traces, the mesh-like patterns and grid are overlaid in the figures to facilitate interpretation of current analytical results.

GWR Model and Results

Ignoring local variations, global linear regression can only generate an overall estimation of the elemental relation, which is obviously against the natural law. Geochemical distributions of ore-forming elements Cu and Au (Fig. 3) are further analyzed

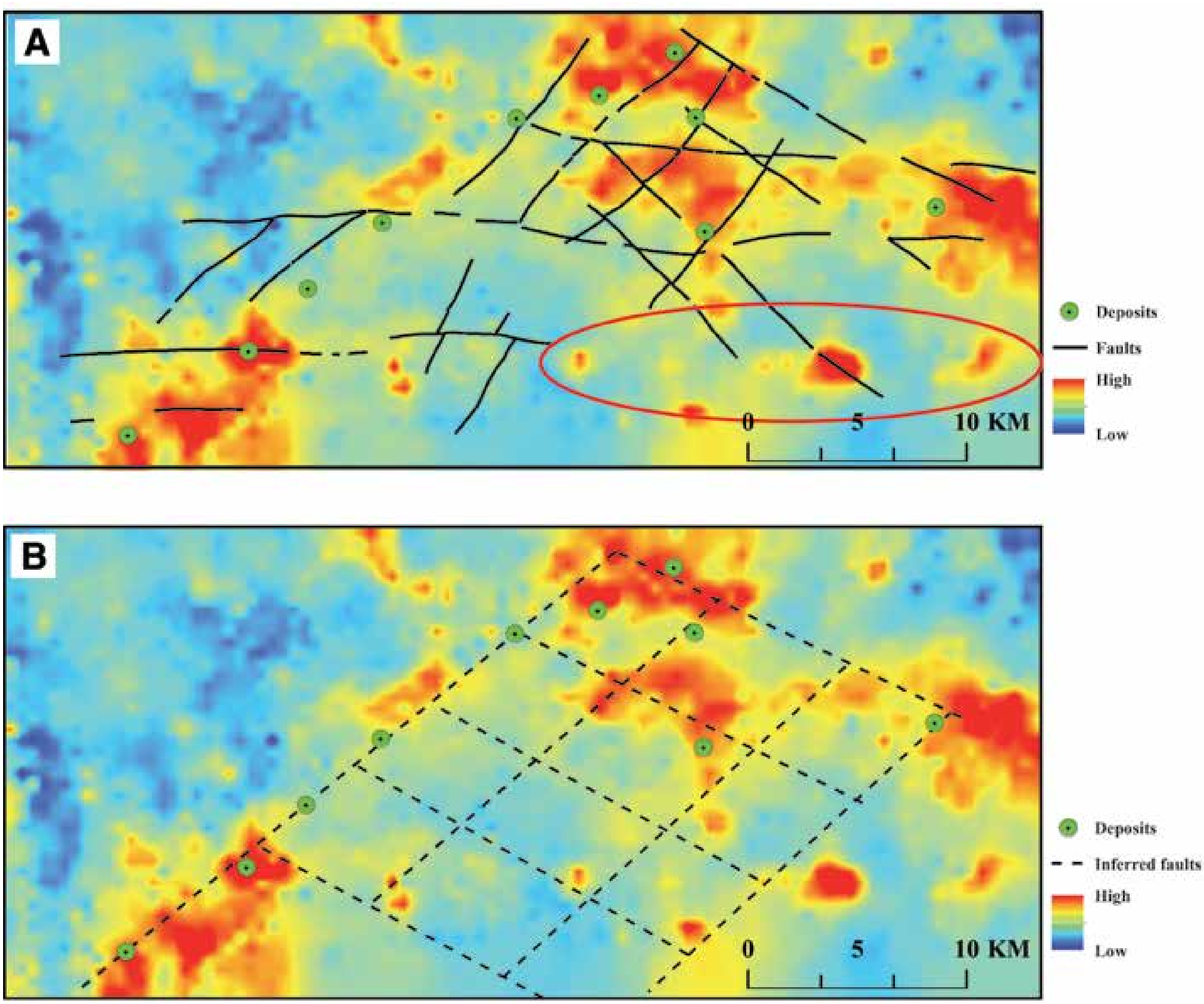

Figure 5. General geochemical background of the Duolong mineral district, Tibet, China, (modified from Liu et al., 2017) is overlapping (A) formerly mapped and (B) interpreted structural frameworks. (C) Student's *t*-values calculated using the weights-of-evidence method for measuring the spatial association between geochemical anomalies and deposits and inferred fault intersections. (D) The value of the *x*-axis with the variable corresponding to the highest *t*-value is considered as the threshold at which to define binary patterns. (*Continued on following page.*)

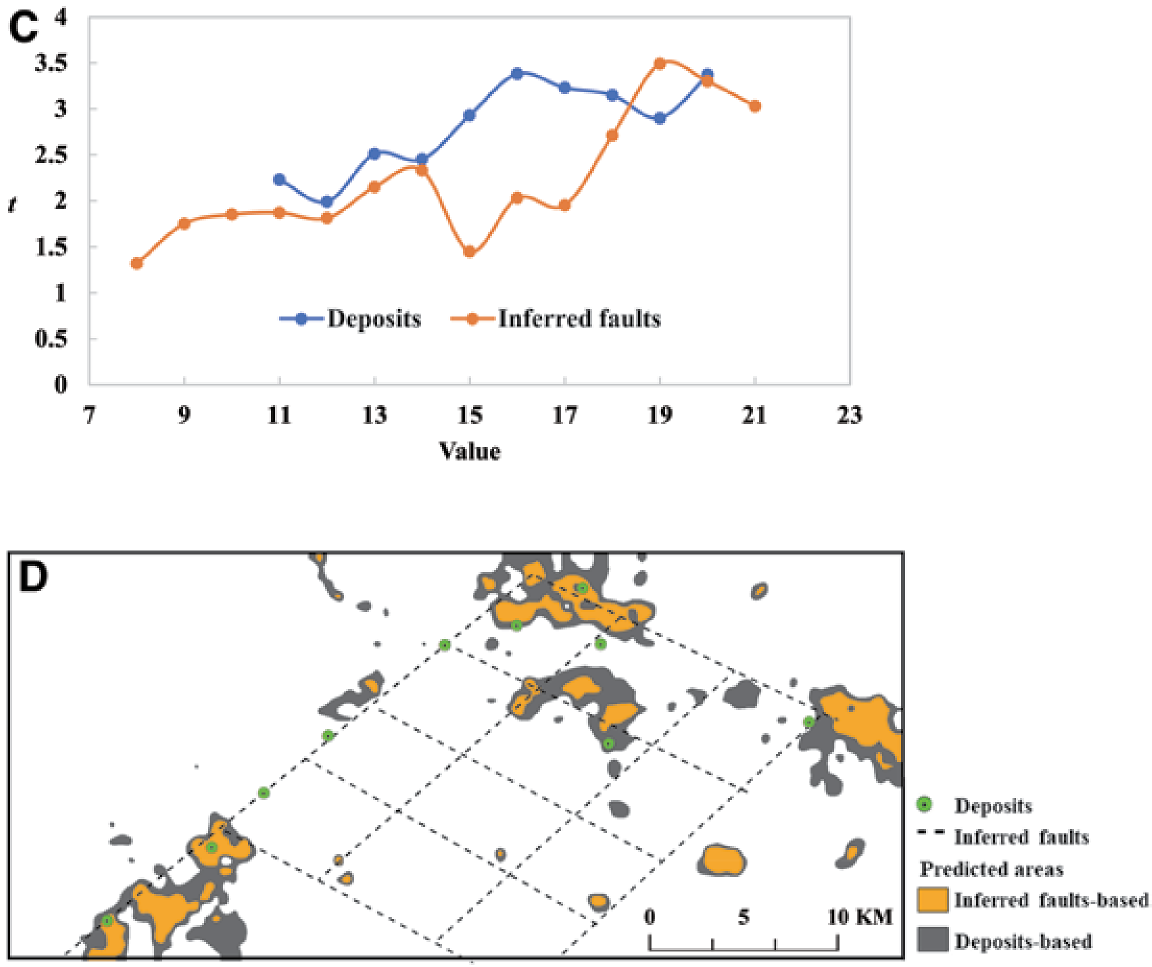

Figure 5 (*Continued*).

using the GWR model to characterize the spatial variation of their paragenetic relation to improve understanding of the local mineralization mechanism within the study area. The GWR model constructed to accomplish this objective can be expressed as follows:

$$Cu_i = \beta_0(u_i, v_i) + \beta_k(u_i, v_i)Au_i + \varepsilon_i, \quad (10)$$

where Cu and Au are defined as dependent and independent variables, respectively. Unlike previous applications of the GWR model (Zhao et al., 2013, 2014; W. Wang et al., 2015a) to investigate the controlling effects of faults, strata, and magmatism on mineralization using local regression coefficients, the model constructed here is intended to obtain the spatial variation of the paragenetic relation between Cu and Au for mineral exploration. The spatial distribution of the regression coefficients $\beta_0(u_i, v_i)$ (Figs. 6A–6B) is more informative with regard to the varied influence of Au on Cu than to their mutual interaction. Meanwhile, the spatially varied coefficient patterns demonstrate and validate the inference discussed above (Fig. 2), i.e., that the paragenetic relation between Cu and Au is complex and varied at different scales across the study area.

The existence of a paragenetic relation can be evaluated and verified using the spatial distribution of local R^2 values (Figs. 6C–6D). Instead of the fixed value produced by the ordinary least squares model, R^2 values generated by the GWR model vary throughout the space, and the higher the value, the stronger the paragenetic relation. Areas with high values of R^2 are consistent with intersections of the mapped and/or interpreted structural framework, which represent spaces with high shear stress that are favorable for porphyry pluton emplacement and porphyry mineralization. Conversely, patterns with low values of R^2 indicate that the paragenetic relation may be weak or that there is no overlap with deposits and fault intersections in such areas. According to the mineralization mechanism, these areas are unsuitable for the formation of porphyry Cu-Au deposits. Generally, the R^2 values from the current GWR model are tenable for examination of the strength of paragenesis between Cu and Au. Additionally, results

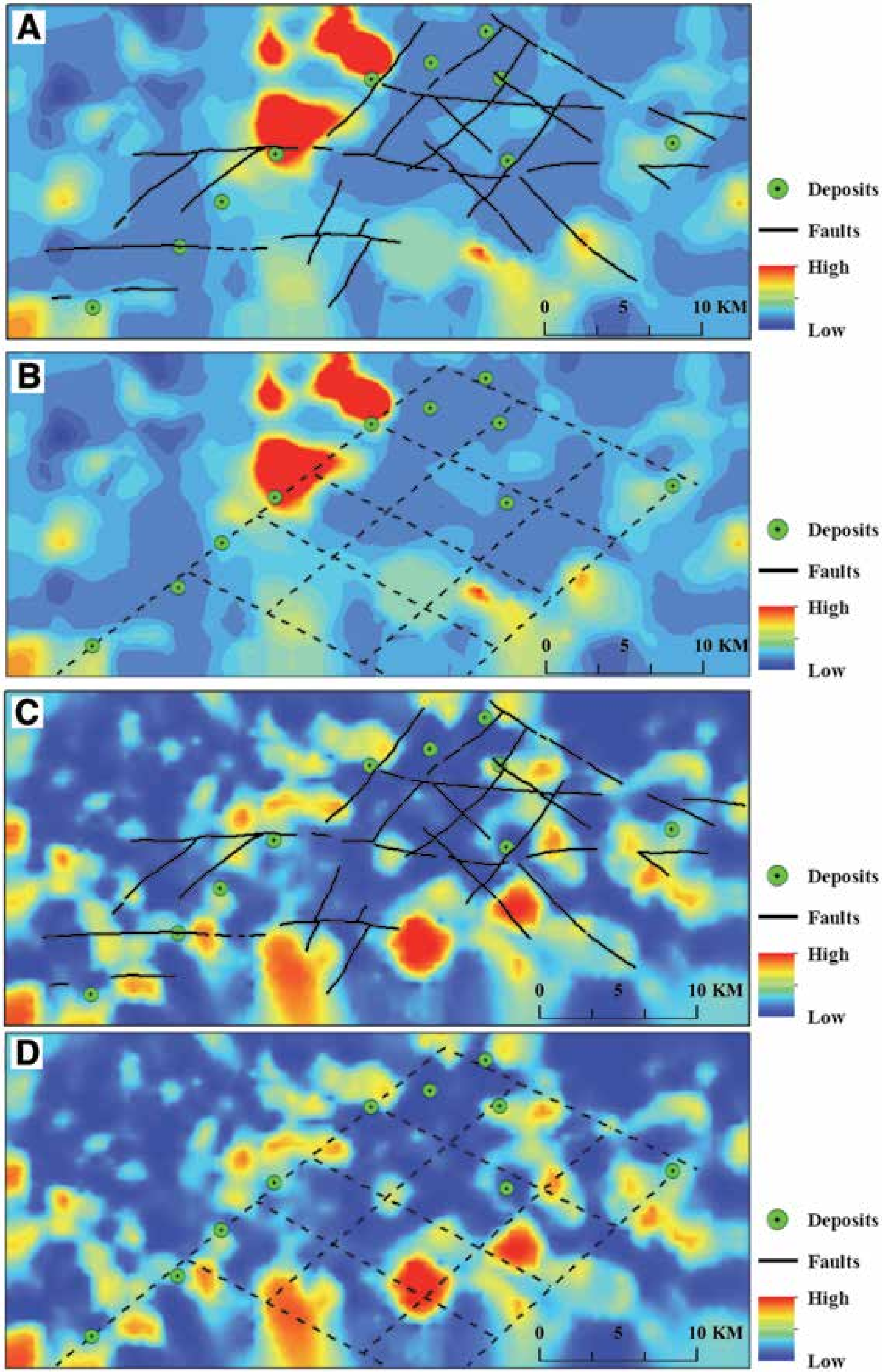

Figure 6. Results produced by the geographically weighted regression (GWR) model (Equation 10) are (A–B) regression coefficients, (C–D) R^2, and (E–F) residuals overlapping formerly mapped (panels A, C, and E) and interpreted (panels B, D, and F) structural frameworks. (*Continued on following page.*)

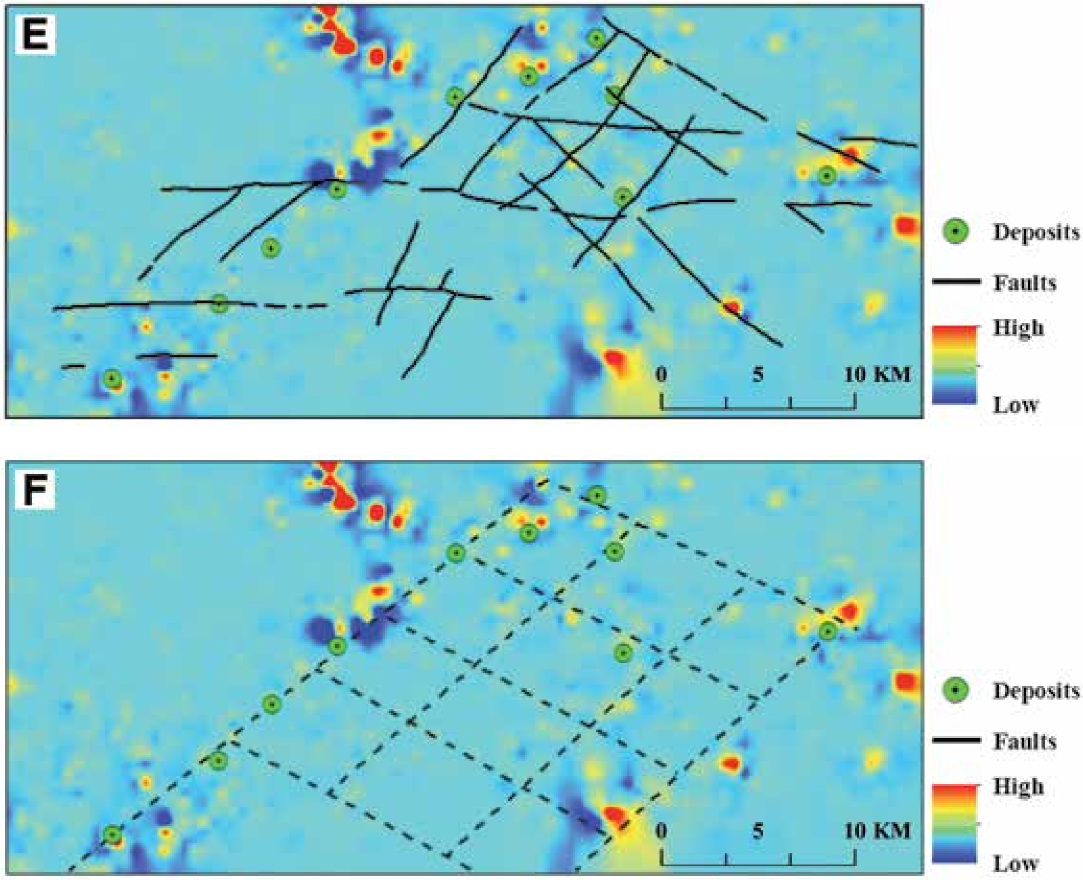

Figure 6 (*Continued*).

also demonstrate the varied paragenetic relation between these two elements across the space with multiple R^2 values, which is in accord with the nonlinear nature of mineralization.

Residuals estimated on the basis of difference between the observed dependent variable and its predicted value are another important parameter regarding interpretation of mineralization. In the current GWR model, high residual values indicate underestimation, while low values correspond to overestimation. Although most residual patterns appear to be randomly distributed (Figs. 6E–6F), use of Moran's *I* index to measure the spatial autocorrelation (Fig. 7) indicates a dispersed distribution, especially for patterns around the intersections of the structural framework. There are two possible reasons for such effects: statistical and geological. The statistical reason is that the current GWR model only investigates two ore-forming elements, and additional accompanying elements of porphyry mineralization or other paragenetic issues of Cu-Au mineralization may need to be considered to improve the precision of the current regression model. Unfortunately, solid phenomenon and geological criteria have not been reported to support such selection. The geological reason is related to the complex and nonlinear mineralization processes. The current GWR model is essentially linear; however, the paragenetic relation discussed in previous studies (figs. 2b–2c in Ulrich et al., 1999) and the Cu-Au metals in boreholes (Fig. 2) are not absolutely linear but may be multilinear or nonlinear. Joint interpretation based on the R^2 values (Figs. 6C–6D) and residuals (Figs. 6E–6F) can only identify areas with a linear paragenetic relation; however, the dispersed residual patterns at the local scale may preserve geoinformation that reflects multilinear and nonlinear issues. Therefore, interpretation of the residual patterns, especially those coincident with known Cu-Au deposits, will always indicate insufficiency of the current GWR model (Equation 10) and the complex paragenetic relation (Figs. 2 and 6A–6B) within these locations. More detailed local exploration and integration of nonlinear regression in the GWR model should be implemented, which would allow for more comprehensive investigation of the paragenetic relations among ore-forming elements.

Data Mining for Mapping Potential Areas

Although it is recognized that insufficiency exists in the model, a general paragenetic relation between Cu and Au can still be delineated and presented as supplementary knowledge with

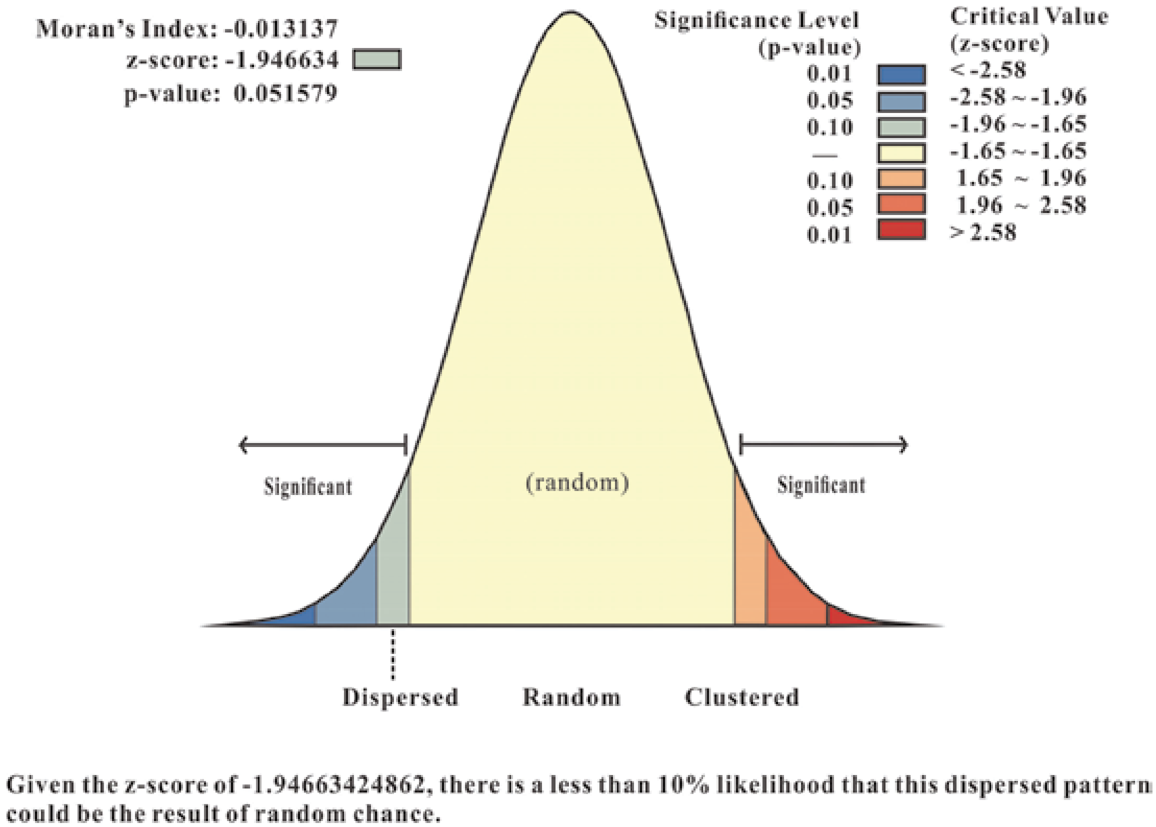

Figure 7. Moran's *I* index was applied to measure the spatial autocorrelation of residual patterns. The chart was modified on the basis of results calculated using ArcGIS software.

regard to realizing new discoveries in the study area. In addition to patterns indicated by spatial distributions of regression coefficients and R^2 values, the current study employs the spectrum–area model to explore finer details of patterns that could identify new target areas. The spatial distributions of local regression coefficients and R^2 values are separated into anomaly and background based on high-pass and band-pass filtering, respectively (Figs. 8–9).

Distinctive patterns can be observed in the background (Figs. 8D–8E) of the regression coefficients $\beta_0(u_i, v_i)$. As highlighted by ellipses, these NE-trending patterns are linearly and equidistantly distributed and spatially consistent with fault intersections at the regional scale; however, they are NW spreading at the local scale if a single ellipse is examined (Figs. 8D–8E). Similar but relatively weak patterns can be found in the eastern and western parts of the study area (highlighted). Overlapping these ellipses on anomaly patterns (Figs. 8B–8C) reveals that several anomalies within these areas are trapped. Referring to the mesh-like structural framework identified through mapping and data mining, anomalous areas indicated by both anomaly (Figs. 8B–8C) and background (Figs. 8D–8E) can be considered areas in which Cu is highly influenced by Au. As discussed above, anomalous patterns interpreted from regression coefficients cannot simply be accepted as a direct indicator of a paragenetic relation without evaluation and verification by R^2. Following the explanation and interpretation of the residuals, only the spatial distribution of R^2 with high values is discussed further with regard to exploration of patterns that indicate mineralization.

Determined by the power spectrum (Fig. 9A), the spatial distribution of R^2 that represents the existence and strength of the paragenetic relation is separated into anomalies (Figs. 9B–9C) and background (Figs. 9D–9E) using high-pass and band-pass filtering, respectively. Geoinformation with high frequency is more indicative of the localized existence of a paragenetic relation, while that with low frequency represents a regional paragenetic relation. Encouraging patterns can be observed in terms of both anomaly and background. Most high values of the anomaly pattern match intersections of the structural framework, which is consistent with the Cu-Au paragenetic relation with high shear stress spaces produced by faults trending in different directions. Meanwhile, weak and inconspicuous patterns in the spatial distribution of R^2 values (Figs. 6C–6D) are markedly enhanced (Fig. 9). By measuring the spatial associations of both anomaly and background patterns with the deposits discovered and inferred fault intersections, the areas indicative of a paragenetic relation can be delineated (Fig. 10). In addition to the areas around

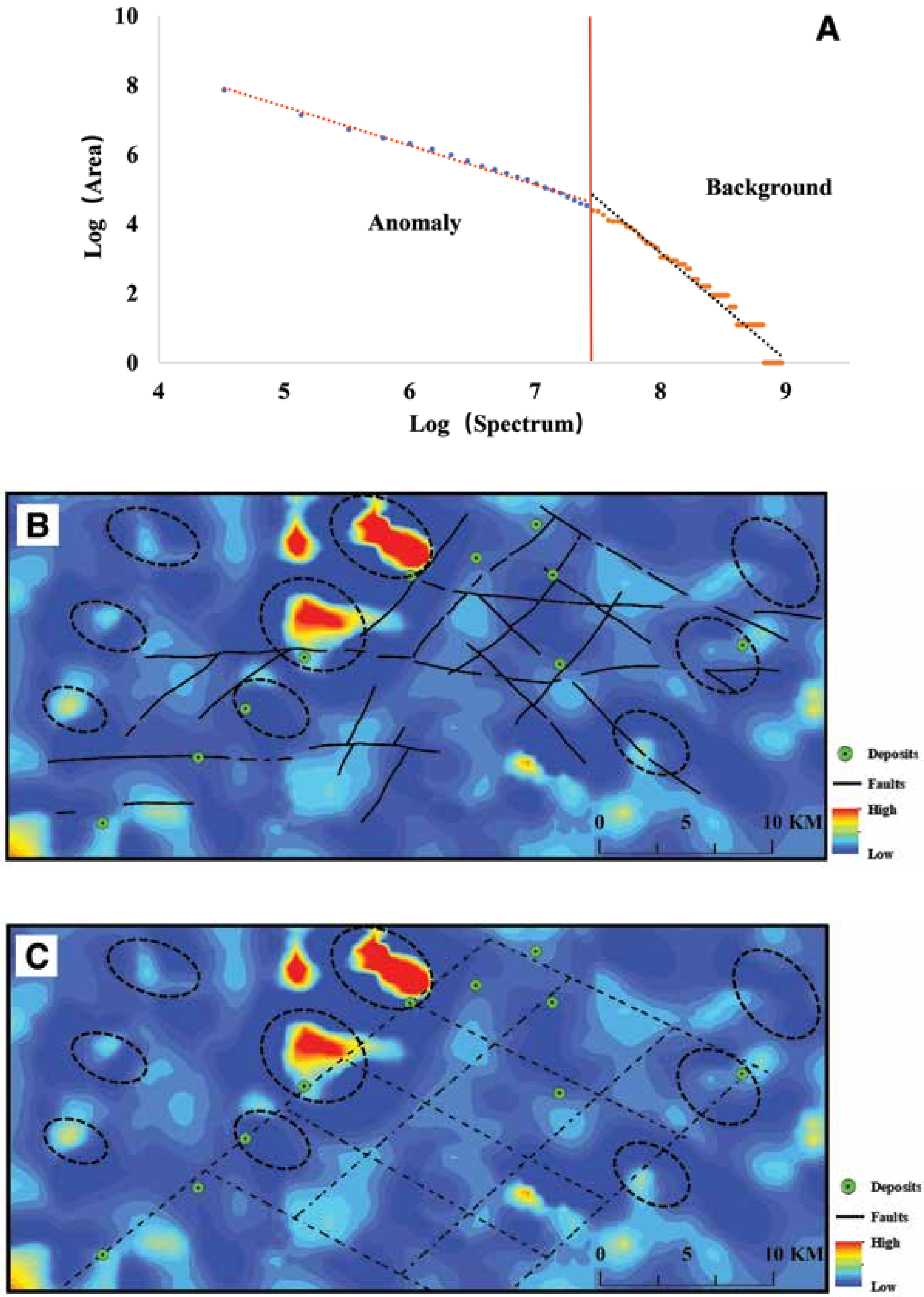

Figure 8. (A) Power spectrum of regression coefficients to define anomaly and background is shown. (B–C) Background and (D–E) anomaly patterns overlapping formerly mapped (panels B and D) and interpreted (panels C and E) structural frameworks (*Continued on facing page.*)

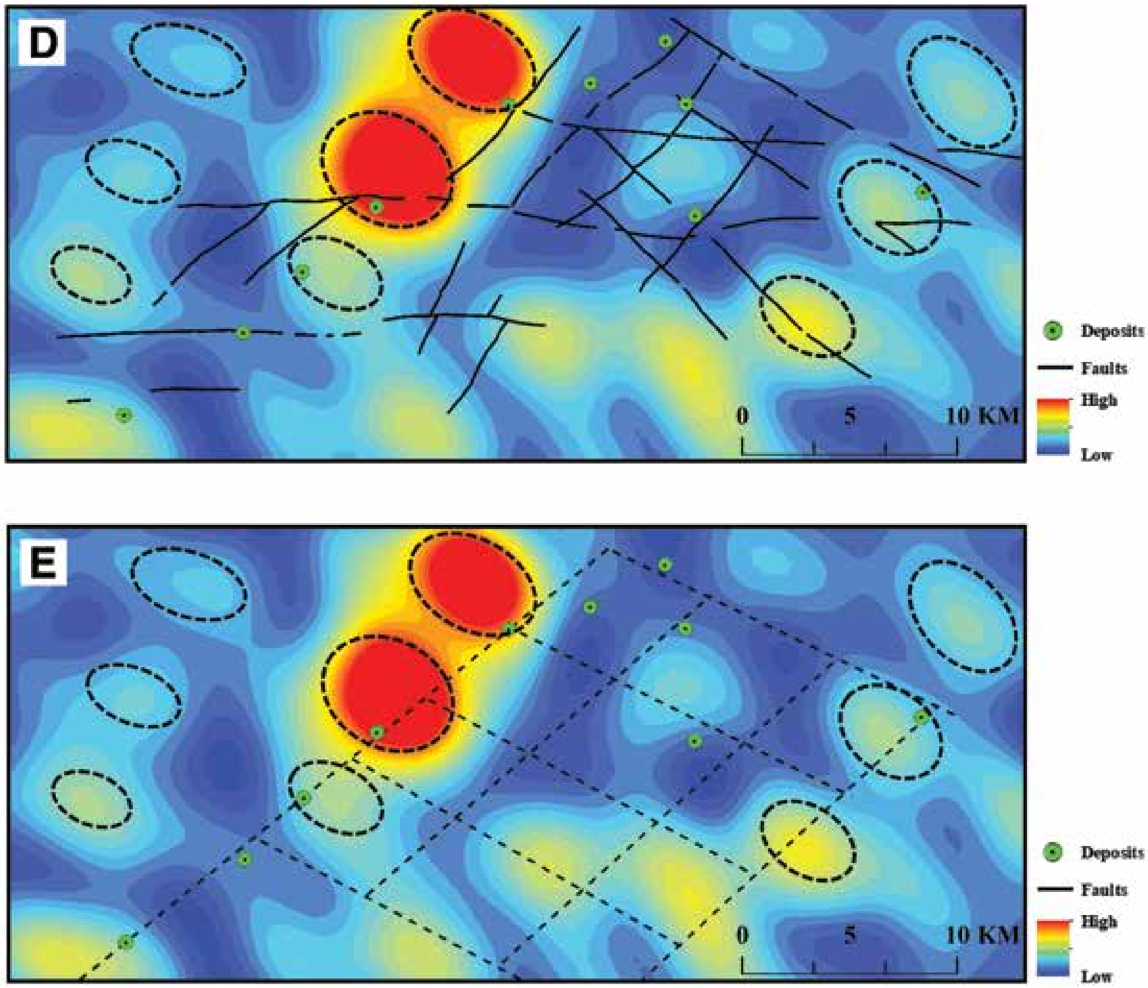

Figure 8 (*Continued*).

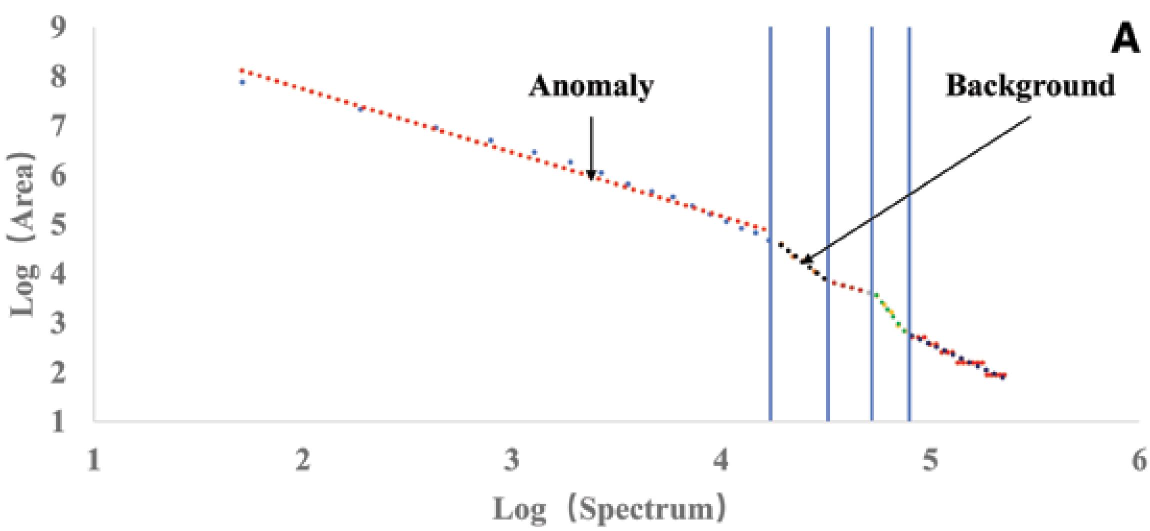

Figure 9. (A) Power spectrum of R^2 to define anomaly and background is shown. (B–C) Background and (D–E) anomaly patterns overlapping formerly mapped (panels B and D) and interpreted (panels C and E) structural frameworks. (*Continued on following page.*)

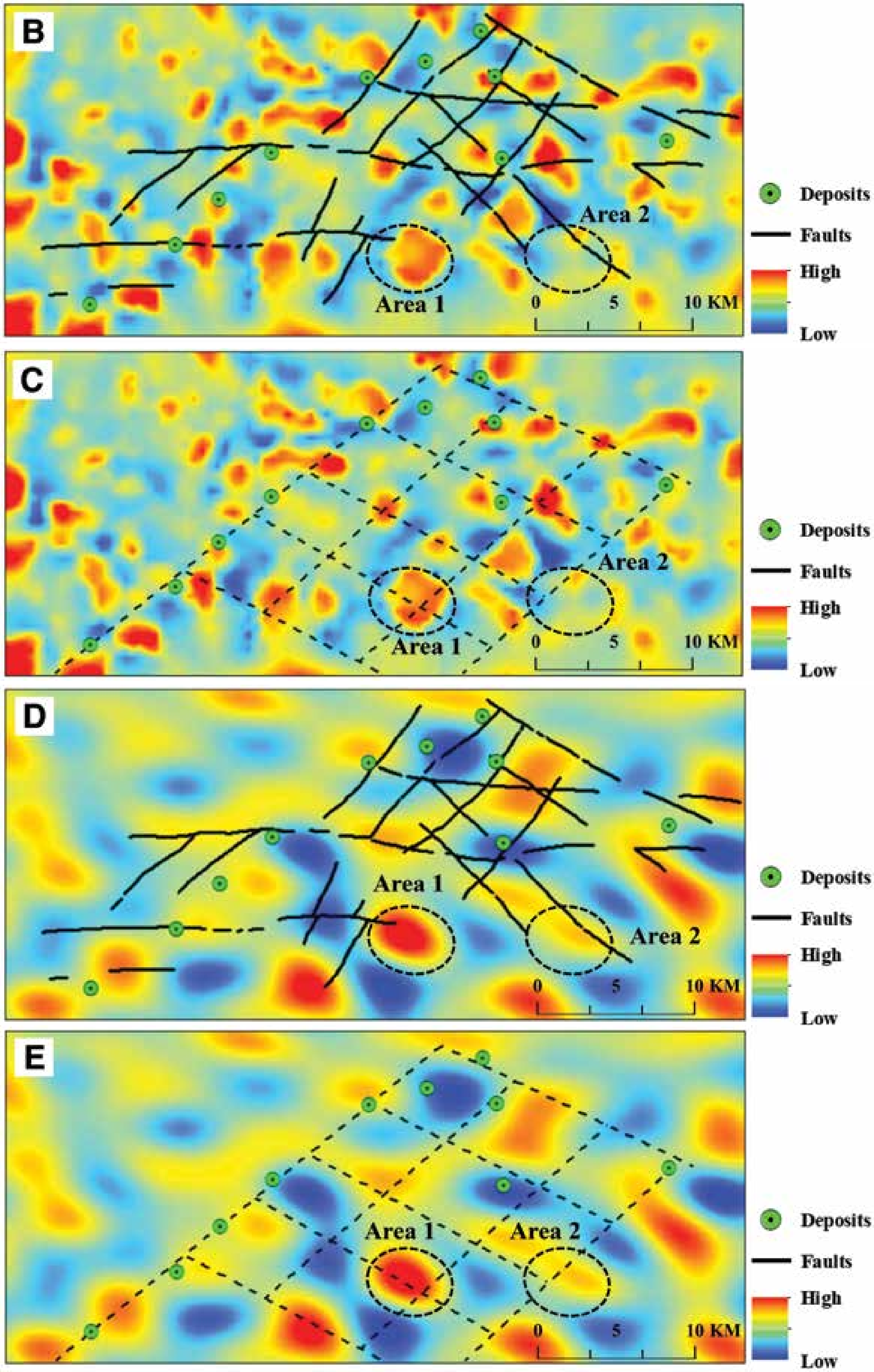

Figure 9 (*Continued*).

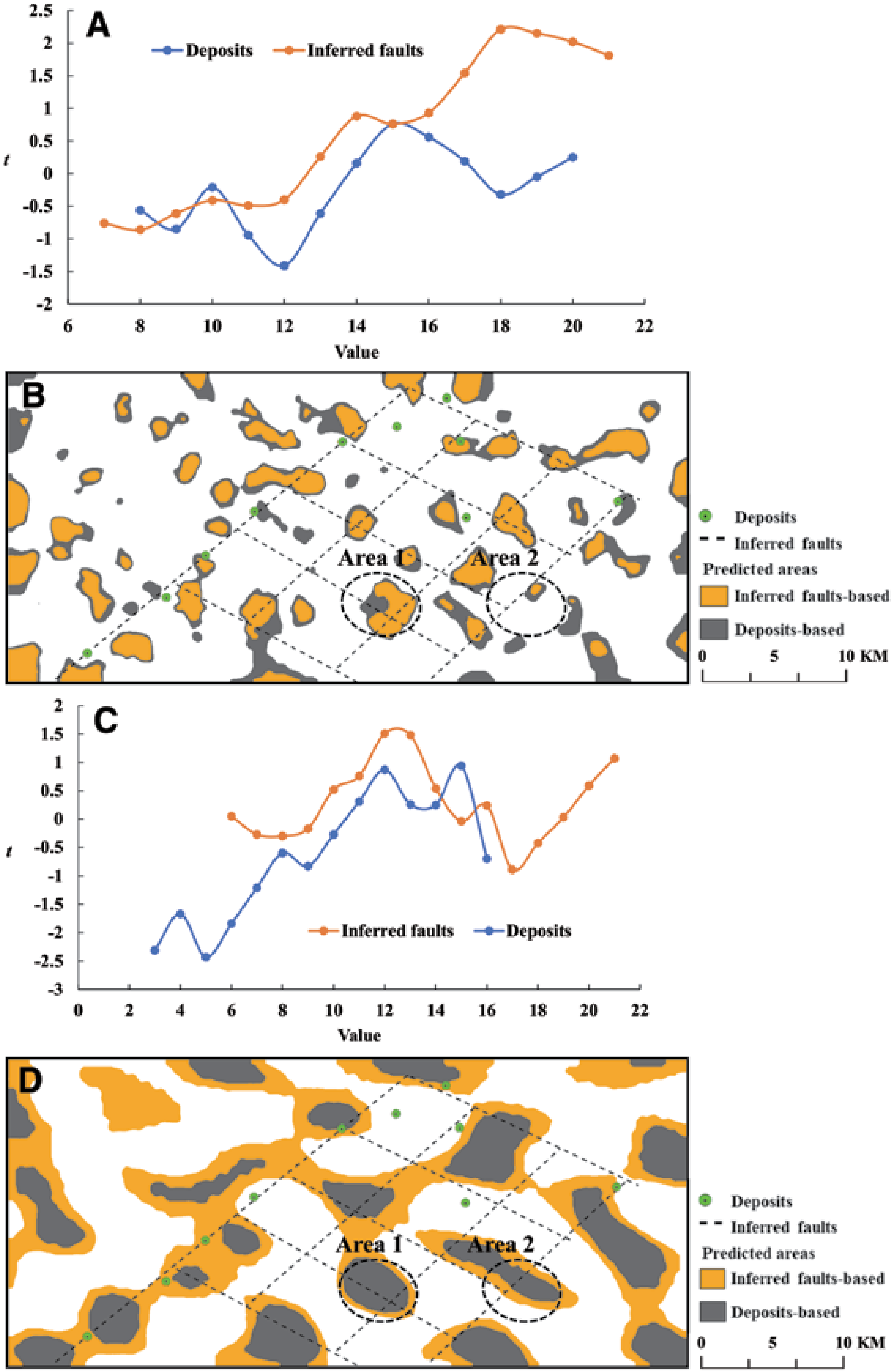

Figure 10. Student's *t*-values were calculated using the weights-of-evidence method for measuring the spatial association of (A–B) anomaly and (C–D) background patterns with deposits and inferred fault intersections. The value of the *x*-axis with the variable corresponding to the highest *t*-value is considered as the threshold at which to define binary patterns (panels B and D).

mineral deposits discovered, anomalous patterns as indicators of a paragenetic relation are trapped and denoted as mineral potential "Area 1" (Figs. 9C and 10B). High values of background patterns are in accord with two structural frameworks, especially the interpreted one (i.e., the mesh-like structural framework) (Figs. 9E and 10D). Similar to the anomaly pattern, an additional potential "Area 2" can be delineated, which is coincident with formerly interpreted and depicted target areas (Fig. 5). Joint review of the GWR results discussed above identifies "Area 2" as the target area for new discoveries, as depicted by both anomaly and the background patterns of the regression coefficients and R^2.

SUMMARY AND DISCUSSION

In modern GIS-based mineral exploration, locating and mapping areas with high mineral potential remain important tasks. However, the current era of big data means that exploiting the advantages of GIS in terms of spatial data management and spatial data mining has never been more important to the discovery of new indicators for recognition of mineralization and related issues. It is imperative that we open our minds and initiate interdisciplinary research regarding new ideas, new methods, and new discoveries. In this chapter, the GWR model, which is commonly used in fields of geography and social science, was employed to investigate the spatial variation of the paragenetic relation between the ore-forming elements Cu and Au in the Duolong mineral district of Tibet, China. As a successor, this study differed from previous applications of GWR to mineral exploration. The objective of earlier work was to investigate the spatially nonstationary controlling effects of geological features on mineralization based on local regression coefficients; thus, R^2 values and residuals were used only to evaluate regression results. To further elucidate the paragenetic relation between ore-forming Cu and Au, which has been discussed in other studies in relation to observations in the Duolong and other porphyry deposits, the current study constructed a GWR model in which Cu and Au were treated as dependent and independent variables, respectively. Given the nature of regression analysis, regression coefficients can represent the influence of the independent variable (Au) on the dependent variable (Cu) but cannot determine whether the relation between these two is paragenetic. Therefore, the current study used R^2, which can assess the regression model, to verify the existence and strength of the paragenetic relation; this constitutes the principal difference between this study and previous work. Furthermore, the fractal- and multifractal-based spectrum–area method was utilized to separate current GWR results (i.e., the R^2 values and regression coefficients) into anomaly and background. Through reference to formerly mapped and interpreted structural frameworks, these GWR and related results were interpreted appropriately. Areas with sufficient R^2 results can be considered as indicators of the existence and strength of the paragenetic relation, which indicates mineralization. Comprehensive interpretation enabled the identification of two target areas with potential for new mineral discoveries.

The current study, which extended scenarios for the application of GWR in mineral exploration, simultaneously addressed some unavoidable issues regarding GWR in the fields of mineral exploration and geology. For example, paragenetic relations such as that between Cu and Au, discussed in this study, are often not statistically significant because of the complex nature of the data and causative factors. Thus, certain meaningful and significant relations have to be excluded to meet statistical conditions, which could limit further development of understanding.

The mineral potential in the Duolong mineral district has been identified by many previous studies. However, the current study not only proposed a new application of GWR for more accurate delineation of target areas, it also aimed to further support the rationality of previously identified target areas from the perspective of the spatial quantitative description of the metallogenic mechanism. Unlike prediction strategies based on comprehensive geoanomaly integration, this research was based on advanced geological theory that used GWR to identify the Cu-Au paragenetic relation. Further optimized by the spatial distribution of R^2, the results obtained were consistent with those of former studies, simultaneously verifying identified target areas and enhancing the theoretical foundation of mineral prediction.

The application of GWR in this study, which used quantitative methods to achieve quantitative recognition of nonlinear issues in mineralization, was a meaningful trial that could represent a useful reference. Moreover, the previously interpreted structural framework was used as supplementary information with regard to recognizing mapped faults for better interpretation of GWR results, although the mesh-like pattern still needs to be verified through geophysical detection. This framework reemphasizes the fact that field-based geological survey and laboratory data analysis are mutually supportive and that both are conducted with the objective of improving geological understanding and thus the success rate of exploration for new discoveries.

ACKNOWLEDGMENTS

The authors sincerely thank Xiaogang (Marshall) Ma for his kind invitation and efforts to organize this GSA Special Paper. We also express our appreciation to our colleagues Xiangchong Liu, Yingru Pei, and Pingping Yu and to graduate students Maoqiang Zhu and Xuerong Ren for their constructive discussion and support. This research was supported by the National Natural Science Foundation of China (grants 41822206 and 41772353).

REFERENCES CITED

Agterberg, F.P., 1989, Computer programs for mineral exploration: Science, v. 245, p. 76–81, https://doi.org/10.1126/science.245.4913.76.

Agterberg, F.P., 2007, Mixtures of multiplicative cascade models in geochemistry: Nonlinear Processes in Geophysics, v. 14, no. 3, p. 201–209, https://doi.org/10.5194/npg-14-201-2007.

Ahrens, L.H., 1953, A fundamental law of geochemistry: Nature, v. 172, no. 1148, https://doi.org/10.1038/1721148a0.

An, P., Moon, W.M., and Rencz, A.N., 1991, Application of fuzzy theory for integration of geological, geophysical and remotely sensed data: Canadian Journal of Exploration Geophysics, v. 27, no. 1, p. 1–11.

Bonham-Carter, G.F., 1994, Geographic Information Systems for Geoscientists: Modelling with GIS. Computer Methods in the Geosciences: New York, Pergamon, 398 p.

Bonham-Carter, G.F., Agterberg, F.P., and Wright, D.F., 1989, Weights of evidence modeling: A new approach to mapping mineral potential, *in* Agterberg, F.P., and Bonham-Carter, G.F., eds., Statistical Applications in the Earth Sciences: Geological Survey of Canada Paper 89, p. 171–183.

Brunsdon, C., Fotheringham, A.S., and Charlton, M.E., 1996, Geographically weighted regression: A method for exploring spatial nonstationarity: Geographical Analysis, v. 28, p. 281–298, https://doi.org/10.1111/j.1538-4632.1996.tb00936.x.

Carranza, E.J.M., 2009, Geochemical Anomaly and Mineral Prospectivity Mapping in GIS: Handbook of Exploration and Environmental Geochemistry 11: Amsterdam, Elsevier Science, 368 p.

Carranza, E.J.M., and Hale, M., 2002, Where are porphyry copper deposits spatially localized? A case study in Benguet province, Philippines: Natural Resources Research, v. 11, p. 45–59, https://doi.org/10.1023/A:1014287720379.

Cheng, Q., 2007, Mapping singularities with stream sediment geochemical data for prediction of undiscovered mineral deposits in Gejiu, Yunnan Province, China: Ore Geology Reviews, v. 32, p. 314–324, https://doi.org/10.1016/j.oregeorev.2006.10.002.

Cheng, Q., 2012, Singularity theory and methods for mapping geochemical anomalies caused by buried sources and for predicting undiscovered mineral deposits in covered areas: Journal of Geochemical Exploration, v. 122, p. 55–70, https://doi.org/10.1016/j.gexplo.2012.07.007.

Cheng, Q., and Agterberg, F.P., 1999, Fuzzy weights of evidence method and its application in mineral potential mapping: Natural Resources Research, v. 8, no. 1, p. 27–35, https://doi.org/10.1023/A:1021677510649.

Cheng, Q., and Agterberg, F.P., 2009, Singularity analysis of ore-mineral and toxic trace elements in stream sediments: Computers & Geosciences, v. 35, p. 234–244, https://doi.org/10.1016/j.cageo.2008.02.034.

Cheng, Q., Agterberg, F.P., and Ballantyne, S.B., 1994, The separation of geochemical anomalies from background by fractal methods: Journal of Geochemical Exploration, v. 51, p. 109–130, https://doi.org/10.1016/0375-6742(94)90013-2.

Cheng, Q., Bonham-Carter, G., Wang, W., Zhang, S., Li, W., and Xia, Q., 2011, A spatially weighted principal component analysis for multi-element geochemical data for mapping locations of felsic intrusions in the Gejiu mineral district of Yunnan, China: Computers & Geosciences, v. 37, p. 662–669, https://doi.org/10.1016/j.cageo.2010.11.001.

Darnley, A.G., 1995, International geochemical mapping—A review: Journal of Geochemical Exploration, v. 55, p. 5–10, https://doi.org/10.1016/0375-6742(95)00035-6.

De Paor, D.G., 1996, Structural Geology and Personal Computers: Oxford, UK, Elsevier, 526 p.

Fan, J., Li, C., Xie, C., and Wang, M., 2014, Petrology, geochemistry, and geochronology of the Zhonggang ocean island, northern Tibet: Implications for the evolution of the Banggongco–Nujiang oceanic arm of the Neo-Tethys: International Geology Review, v. 56, p. 1504–1520, https://doi.org/10.1080/00206814.2014.947639.

Fotheringham, A.S., Brunsdon, C., and Charlton, M., 2002, Geographically Weighted Regression: The Analysis of Spatially Varying Relationships: Chichester, UK, Wiley, 282 p.

Ghil, M., 2019, A century of nonlinearity in the geosciences: Earth and Space Science, v. 6, p. 1007–1042, https://doi.org/10.1029/2019EA000599.

Grunsky, E.C., 1986, Recognition of alteration in volcanic rocks using statistical analysis of lithogeochemical data: Journal of Geochemical Exploration, v. 25, p. 157–183, https://doi.org/10.1016/0375-6742(86)90012-9.

Grunsky, E.C., and Smee, B.W., 1999, The differentiation of soil types and mineralization from multi-element geochemistry using multivariate methods and digital topography: Journal of Geochemical Exploration, v. 67, p. 287–299, https://doi.org/10.1016/S0375-6742(99)00054-0.

Grunsky, E.C., Drew, L.J., and Sutphin, D.M., 2009, Process recognition in multi-element soil and stream-sediment geochemical data: Applied Geochemistry, v. 24, p. 1602–1616, https://doi.org/10.1016/j.apgeochem.2009.04.024.

Grunsky, E.C., Mueller, U.A., and Corrigana, D., 2014, A study of the lake sediment geochemistry of the Melville Peninsula using multivariate methods: Applications for predictive geological mapping: Journal of Geochemical Exploration, v. 141, p. 15–41, https://doi.org/10.1016/j.gexplo.2013.07.013.

Haldar, S.K., 2018, Mineral Exploration: Principles and Applications: Oxford, UK, Elsevier, 378 p.

Harris, D., Zurcher, L., Stanley, M., Marlow, J., and Pan, G., 2003, A comparative analysis of favorability mappings by weights of evidence, probabilistic neural networks, discriminant analysis, and logistic regression: Natural Resources Research, v. 12, no. 4, p. 241–255, https://doi.org/10.1023/B:NARR.0000007804.27450.e8.

Hogson, C.J., 1990, Uses (and abuses) of ore deposit models in mineral exploration: Geoscience Canada, v. 17, p. 79–89.

Hou, Z., Mo, X., Yang, Z., Wang, A., Pan, G., Qu, X., and Nie, F., 2006, Metallogeneses in the collisional orogeny of the Qinghai-Tibet Plateau: Tectonic setting, tempo-spatial distribution and ore deposit types: Geology in China, v. 33, p. 340–351 [in Chinese with English abstract].

Li, C., Ma, T., and Shi, J., 2003, Application of a fractal method relating concentrations and distances for separation of geochemical anomalies from background: Journal of Geochemical Exploration, v. 77, p. 167–175, https://doi.org/10.1016/S0375-6742(02)00276-5.

Li, Q., and Cheng, Q., 2004, Multifractal singular value decomposition and reconstruction of geochemical and geophysical data: Journal of China University of Geosciences, v. 29, p. 109–118 [in Chinese with English abstract and illustrations].

Li, X., Li, C., Sun, Z., and Wang, M., 2017, Origin and tectonic setting of the giant Duolong Cu–Au deposit, South Qiangtang terrane, Tibet: Evidence from geochronology and geochemistry of Early Cretaceous intrusive rocks: Ore Geology Reviews, v. 80, p. 61–78, https://doi.org/10.1016/j.oregeorev.2016.06.025.

Lin, B., Tang, J., Chen, Y., Baker, M., Song, Y., Yang, H., Wang, Q., He, W., and Liu, Z., 2019, Geology and geochronology of Naruo large porphyry-breccia Cu deposit in the Duolong district, Tibet: Gondwana Research, v. 66, p. 168–182, https://doi.org/10.1016/j.gr.2018.07.009.

Liu, X., Wang, W., Pei, Y., and Yu, P., 2020, A knowledge-driven way to interpret the isometric log-ratio transformation and mixture distributions of geochemical data: Journal of Geochemical Exploration, v. 210, https://doi.org/10.1016/j.gexplo.2019.106417.

Liu, Z., Wang, W., Song, Y., and Wang, Q., 2017, Geo-information extraction and integration of ore-controlling structure in the Duolong ore concentration area of Tibet: Acta Geoscientica Sinica, v. 38, no. 5, p. 803–812 [in Chinese with English abstract and illustrations].

Lu, B., Charlton, M., Harris, P., and Fotheringham, A.S., 2014, Geographically weighted regression with a non-Euclidean distance metric: A case study using hedonic house price data: International Journal of Geographical Information Science, v. 28, no. 4, p. 660–681, https://doi.org/10.1080/13658816.2013.865739.

Lu, B., Ge, Y., Qin, K., and Zheng, J., 2020, A review on geographically weighted regression: Wuhan Daxue Xuebao (Xinxi Kexue Ban), v. 45, no. 9, p. 1356–1366 [in Chinese with English abstract and illustrations].

Madani, N., and Carranza, E.J.M., 2020, Co-simulated size number: An elegant novel algorithm for identification of multivariate geochemical anomalies: Natural Resources Research, v. 29, p. 13–40, https://doi.org/10.1007/s11053-019-09547-9.

Madani, N., and Sadeghi, B., 2019, Capturing hidden geochemical anomalies in scarce data by fractal analysis and stochastic modeling: Natural Resources Research, v. 28, p. 833–847, https://doi.org/10.1007/s11053-018-9421-4.

Mandelbrot, B.B., 1983, The Fractal Geometry of Nature: San Francisco, California, Freeman, 468 p., https://doi.org/10.1119/1.13295.

Mayer-Schönberger, V., and Cukier, K., 2013, Big Data: A Revolution That Will Transform How We Live, Work, and Think: New York, Houghton Mifflin Harcourt, 242 p.

Pan, G., Wang, L., Li, R., Yuan, S., Ji, W., Yin, F., Zhang, W., and Wang, B., 2012, Tectonic evolution of the Qinghai-Tibet Plateau: Journal of Asian Earth Sciences, v. 53, p. 3–14, https://doi.org/10.1016/j.jseaes.2011.12.018.

Pirajno, F., 2009, Hydrothermal Processes and Mineral Systems: Berlin, Springer, 1250 p., https://doi.org/10.1007/978-1-4020-8613-7.

Sadeghi, B., and Cohen, D.R., 2021a, Concentration-distance from centroids (C-DC) multifractal modeling: A novel approach to characterizing geochemical patterns based on sample distance from mineralization: Ore Geology Reviews, v. 137, https://doi.org/10.1016/j.oregeorev.2021.104302.

Sadeghi, B., and Cohen, D.R., 2021b, Category-based fractal modelling: A novel model to integrate the geology into the data for more effective processing and interpretation: Journal of Geochemical Exploration, v. 226, https://doi.org/10.1016/j.gexplo.2021.106783.

Sadeghi, B., Yilmaz, H., and Pirajno, F., 2021, Weighting of BLEG data with drainage and catchment properties to enhance Au anomalies: Geochemistry, v. 81, https://doi.org/10.1016/j.chemer.2020.125733.

Segall, P., and Pollard, D.D., 1980, Mechanics of discontinuous faults: Journal of Geophysical Research: Solid Earth, v. 85, p. 4337–4350, https://doi.org/10.1029/JB085iB08p04337.

Song, Y., Yang, C., Wei, S., Yang, H., Fang, X., and Lu, H., 2018, Tectonic control, reconstruction and preservation of the Tiegelongnan porphyry and epithermal overprinting Cu (Au) deposit, central Tibet, China: Minerals, v. 8, no. 9, https://doi.org/10.3390/min8090398.

Tu, J., and Xia, Z., 2008, Examining spatially varying relationships between land use and water quality using geographically weighted regression I: Model design and evaluation: The Science of the Total Environment, v. 407, no. 1, p. 358–378, https://doi.org/10.1016/j.scitotenv.2008.09.031.

Ulrich, T., Günther, D., and Heinrich, C.A., 1999, Gold concentrations of magmatic brines and the metal budget of porphyry copper deposits: Nature, v. 399, no. 6737, p. 676–679, https://doi.org/10.1038/21406.

Wang, H., Cheng, Q., and Zuo, R., 2015, Quantifying the spatial characteristics of geochemical patterns via GIS-based geographically weighted statistics: Journal of Geochemical Exploration, v. 157, p. 110–119, https://doi.org/10.1016/j.gexplo.2015.06.004.

Wang, W., Zhao, J., and Cheng, Q., 2011, Analysis and integration of geo-information to identify granitic intrusions as exploration targets in southeastern Yunnan District, China: Computers & Geosciences, v. 37, p. 1946–1957, https://doi.org/10.1016/j.cageo.2011.06.023.

Wang, W., Zhao, J., and Cheng, Q., 2015, GIS-based mineral exploration modeling by advanced geo-information analysis methods in southeastern Yunnan mineral district, China: Ore Geology Reviews, v. 71, p. 735–748, https://doi.org/10.1016/j.oregeorev.2014.09.032.

Wang, W., Cheng, Q., Tang, J., Pubuciren, Song, Y., Li, Y., and Liu, Z., 2017, Fractal and multifractal analysis in support of mineral exploration in the Duolong mineral district, Tibet, China: Geochemistry Exploration Environment Analysis, v. 17, p. 261–276, https://doi.org/10.1144/geochem2016-449.

Wang, W., Cheng, Q., Zhang, S., and Zhao, J., 2018, Anisotropic singularity: A novel way to characterize controlling effects of geological processes on mineralization: Journal of Geochemical Exploration, v. 189, p. 32–41, https://doi.org/10.1016/j.gexplo.2017.07.019.

Woodall, R., 1994, Empiricism and concept in successful mineral exploration: Australian Journal of Earth Sciences, v. 41, p. 1–10.

Xie, S., and Bao, Z., 2004, Fractal and multifractal properties of geochemical fields: Mathematical Geology, v. 36, no. 7, p. 847–864, https://doi.org/10.1023/B:MATG.0000041182.70233.47.

Xu, M., Li, C., Zhang, X., and Wu, Y., 2014, Nature and evolution of the Neo-Tethys in central Tibet: Synthesis of ophiolitic petrology, geochemistry, and geochronology: International Geology Review, v. 56, p. 1072–1096, https://doi.org/10.1080/00206814.2014.919616.

Xu, Y., and Cheng, Q., 2001, A fractal filtering technique for processing regional geochemical maps for mineral exploration: Geochemistry Exploration Environment Analysis, v. 1, p. 147–156, https://doi.org/10.1144/geochem.1.2.147.

Yu, P., Chen, J., and Wang, Q., 2019, Three-dimensional mineral prospectivity modelling and deep metallogenic prediction of the Tiegelongnan copper-gold deposit in Tibet, China: Yanshi Xuebao, v. 35, no. 3, p. 897–912.

Zhang, Z., Yao, X., Tang, J., Li, Z., Wang, L., Yang, Y., Duan, J., Song, J., and Lin, X., 2015, Lithogeochemical, Re-Os and U-Pb geochronological, Hf-Lu and S-Pb isotope data of the Ga'erqiong-Galale Cu-Au Ore-concentrated area: Evidence for the Late Cretaceous magmatism and metallogenic event in the Bangong-Nujiang suture zone, Northwestern Tibet, China: Resource Geology, v. 65, p. 76–102, https://doi.org/10.1111/rge.12064.

Zhao, J., Wang, W., Dong, L., Yang, W., and Cheng, Q., 2012, Application of geochemical anomaly identification methods in mapping of intermediate and felsic igneous rocks in eastern Tianshan, China: Journal of Geochemical Exploration, v. 122, p. 81–89, https://doi.org/10.1016/j.gexplo.2012.08.006.

Zhao, J., Wang, W., and Cheng, Q., 2013, Investigation of spatially non-stationary influences of tectono-magmatism on Fe mineralization in eastern Tianshan, China with geographically weighted regression: Journal of Geochemical Exploration, v. 134, p. 38–50, https://doi.org/10.1016/j.gexplo.2013.07.008.

Zhao, J., Wang, W., and Cheng, Q., 2014, Application of geographically weighted regression to identify spatially non-stationary relationships between Fe mineralization and its controlling factors in eastern Tianshan, China: Ore Geology Reviews, v. 57, p. 628–638, https://doi.org/10.1016/j.oregeorev.2013.08.005.

Zhao, J., Wang, W., Cheng, Q., and Agterberg, F., 2016, Mapping of Fe mineral potential by spatially weighted principal component analysis in the eastern Tianshan mineral district, China: Journal of Geochemical Exploration, v. 164, p. 107–121, https://doi.org/10.1016/j.gexplo.2015.11.004.

Zhu, D., Li, S., Cawood, P., Wang, Q., Zhao, Z., Liu, S., and Wang, L., 2016, Assembly of the Lhasa and Qiangtang terranes in central Tibet by divergent double subduction: Lithos, v. 245, p. 7–17, https://doi.org/10.1016/j.lithos.2015.06.023.

Zuo, R., 2020, Geodata science-based mineral prospectivity mapping: A review: Natural Resources Research, v. 29, p. 3415–3424, https://doi.org/10.1007/s11053-020-09700-9.

Zuo, R., Cheng, Q., Xia, Q., and Agterberg, F.P., 2009, Application of singularity mapping technique to identify local anomalies using stream sediment geochemical data, a case study from Gangdese, Tibet, western China: Journal of Geochemical Exploration, v. 101, p. 225–235, https://doi.org/10.1016/j.gexplo.2008.08.003.

Zuo, R., Xiong, Y., Wang, J., and Carranza, E.J.M., 2019, Deep learning and its application in geochemical mapping: Earth-Science Reviews, v. 192, p. 1–14, https://doi.org/10.1016/j.earscirev.2019.02.023.

Manuscript Accepted by the Society 17 March 2022
Manuscript Published Online 12 September 2022

Printed in the USA